MOLECULAR AND CELLULAR BIOLOGY, Apr. 1996, p. 1857–1870 Vol. 16, No. 4
0270-7306/96/$04.00+0

Genetic Analysis of the Bipolar Pattern of Bud Site Selection in the Yeast *Saccharomyces cerevisiae*

JOSEPH E. ZAHNER, HEIDI A. HARKINS, AND JOHN R. PRINGLE*

Department of Biology, University of North Carolina, Chapel Hill, North Carolina 27599

Received 24 October 1995/Returned for modification 27 November 1995/Accepted 5 January 1996

Previous analysis of the bipolar budding pattern of *Saccharomyces cerevisiae* has suggested that it depends on persistent positional signals that mark the region of the division site and the tip of the distal pole on a newborn daughter cell, as well as each previous division site on a mother cell. In an attempt to identify genes encoding components of these signals or proteins involved in positioning or responding to them, we identified 11 mutants with defects in bipolar but not in axial budding. Five mutants displaying a bipolar budding-specific randomization of budding pattern had mutations in four previously known genes (*BUD2*, *BUD5*, *SPA2*, and *BNI1*) and one novel gene (*BUD6*), respectively. As Bud2p and Bud5p are known to be required for both the axial and bipolar budding patterns, the alleles identified here probably encode proteins that have lost their ability to interact with the bipolar positional signals but have retained their ability to interact with the distinct positional signal used in axial budding. The function of Spa2p is not known, but previous work has shown that its intracellular localization is similar to that postulated for the bipolar positional signals. *BNI1* was originally identified on the basis of genetic interaction with *CDC12*, which encodes one of the neck-filament-associated septin proteins, suggesting that these proteins may be involved in positioning the bipolar signals. One mutant with a heterogeneous budding pattern defines a second novel gene (*BUD7*). Two mutants budding almost exclusively from the proximal pole carry mutations in a third novel gene (*BUD8*), and three mutants budding exclusively from the distal pole carry mutations in a fourth novel gene (*BUD9*). A *bud8 bud9* double mutant also buds almost exclusively from the proximal pole, suggesting that Bud9p is involved in positioning the proximal-pole signal rather than being itself a component of this signal.

The establishment of cell polarity is a central feature of morphogenesis in many types of cells, and an important aspect of this process is the selection of an appropriate axis of polarization. In the budding yeast *Saccharomyces cerevisiae*, cell polarity is manifested during the vegetative cell cycle by the appearance and selective growth of the bud, which involves a polarization of secretion and cell surface growth dependent on an underlying polarization of the cytoskeleton; this polarization is dependent on a set of "polarity-establishment functions" that include the GTPase Cdc42p and its activating factor Cdc24p (10, 14, 21, 31, 56, 72). The axes of polarization (i.e., bud sites) are typically selected in either of two patterns, depending on cell type. **a** or α cells (e.g., normal haploids) typically use the axial pattern, in which both mother and daughter cells bud adjacent to the preceding division site, whereas **a**/α cells (e.g., normal diploids) typically bud in the bipolar pattern, in which the daughter cell generally buds at the pole distal to the division site and the mother cell can bud near either pole (28, 36, 68, 71, 73). Both budding patterns depend on a set of "general site selection functions" that make up a functional GTPase module. *RSR1* (or *BUD1*) encodes a Ras-related, low-molecular-weight GTPase (4), whereas *BUD2* and *BUD5* encode a GTPase-activating protein and guanine nucleotide exchange factor, respectively, that act on Rsr1p (3, 11, 12, 53, 54, 62, 74). Null mutations in any of these three genes cause random budding irrespective of cell type.

A recent detailed analysis of the two budding patterns suggested that the axial pattern depends on a transient positional signal that marks the division site on both mother and daughter cells (15). The products of the *BUD3* and *BUD4* genes, which were identified originally on the basis of mutations that affect the axial but not the bipolar budding pattern (12), appear to be components of this transient signal (13, 65). In contrast, the bipolar pattern appears to depend on persistent or permanent positional signals that mark the region of the division site and the tip of the distal pole on a newborn daughter cell, as well as each previously used division site on a mother cell (15). It seemed likely that genes encoding components of these positional signals or proteins involved in positioning or responding to them could be identified by analyzing mutants defective in bipolar but not in axial budding. We report here the isolation and analysis of 11 such mutants.

MATERIALS AND METHODS

Strains, media, growth conditions, and genetic techniques. *Escherichia coli* DH5α was used for plasmid maintenance by following standard procedures (64). *S. cerevisiae* strains and plasmids used in this study are described in Table 1. Yeast cultures were grown at 30°C except where otherwise noted. The solid media used were YPD rich medium, synthetic complete (SC) medium, SC medium lacking particular nutrients (SC-His, SC-Leu, etc.), and minimal synthetic sporulation medium supplemented with amino acids, all made as described previously (61). Liquid cultures were grown in YM-P rich medium containing 2% glucose (48). Mating types were determined by crossing to tester strains CMB102 and JC08B and scoring the formation of prototrophs. For crosses, matings were carried out either by isolating zygotes by micromanipulation after 4 h of mating or by streaking out an overnight mating reaction and picking larger colonies. Diploids were confirmed by the ability to sporulate and the inability to mate. Sporulation and tetrad analysis were performed by standard procedures (66). Transformations were done by the lithium acetate method (38).

Mutagenesis. For UV mutagenesis, strain 486 was grown to stationary phase in YM-P medium. Cells were counted with a hemocytometer and plated to give ~3,500 cells per 10-cm-diameter YPD plate. The plates were then subjected to shortwave UV radiation for various times to generate a killing curve; 99% killing was produced by 40 s of exposure. For the mutant screen, ~10,000 cells were

* Corresponding author. Mailing address: Department of Biology, CB #3280—Coker Hall, University of North Carolina, Chapel Hill, NC 27599-3280. Phone: (919) 962-2293. Fax: (919) 962-0320.

TABLE 1. Yeast strains and plasmids used in this study

Strain or plasmid	Genotype or description	Source or reference
Strains		
52	**a**/α *his4/his4 trp1/trp1 ura3/ura3*	12
124	α *his4 trp1 ura3 bud2-1*	12
191	**a** *his4 trp1 ura3 bud4-1*	Similar to strain 135 (12)
206	α *his4 trp1 ura3 bud5::URA3*	Similar to strain 205 (11)
486	α *his4 trp1 ura3 bud3::TRP1*	13
1237-1	**a** *his4 trp1 ura3*	12
1237-13C	α *his4 trp1 ura3*	12
1241-2D	**a** *leu2 trp1 ura3*	12
12021	**a** *ade1 ade2 his7 lys2 tyr1 ura1 cdc31-1*	34
A3-2D	**a** *trp1 ura3 sur4::URA3*	20, 24, 25
BR205-2	**a** *ade2 arg4 his7 trp1 ura1 cdc25-2*	39
C82-1857	**a** *arg1 asp5 ilv5 met1 ura4*	YGSC[a]
CMB102	**a** *met1*	Pringle lab collection
HP24	**a** *ade2 his3 leu2 lys2 trp1 ura3 bud2Δ::LEU2*	Similar to strain HP25 (53)
JC08B	α *met1*	Pringle lab collection
JF17	α *ade2 his3 leu2 lys2 trp1 ura3 bni1::LEU2*	26
JF23	**a**/α *his4/his4 trp1/trp1 ura3/ura3 bni1::URA3/bni1::URA3*	26
L181-6B	α *leu2 trp1 ura3 dbf2-2*	L. Johnston
LG70-7A	**a** *trp1 ura3 fen1::URA3*	24, 25
M-154	**a** *ade2 ade3 leu2 lys2 trp1 ura3 cdc3-1*	M. Longtine
MM5.4	α *his4 trp1 ura3 bud3::URA3*	13
S2072A	**a** *arg4 leu1 trp1*	YGSC
SLY254	**a** *ura3 myo2-66*	S. Lillie and S. Brown[b]
Y147	**a** *his3 leu2 ura3 cdc24-4*	4
Y301	α *his3 leu2 ura3 rsr1::URA3*	4
Y548	α *his3 leu2 trp1 ura3 kss1::HIS3 msb2::URA3 rme1::lacZ*	6
Y601	α *ade2 his3 lys2 trp1 ura3 spa2-Δ3::URA3*	30
Y609	**a** *ade2 his3 lys2 trp1 ura3 spa2-Δ2::TRP1*	30
Y650	**a**/α *ade2/ade2 his3/his3 lys2/lys2 trp1/trp1 ura3/ura3 spa2-Δ2::TRP1/spa2-Δ3::URA3*	30
YHH16	**a** *leu2 trp1 ura3 bud3::TRP1*	This study[c]
YHH76	**a** *his4 trp1 ura3 bud3::TRP1 bud9-2*	This study[d]
YHH77	α *his4 trp1 ura3 bud3::TRP1 bud9-2*	This study[d]
YHH81	α *his4 trp1 ura3 bud3::TRP1 bud7-1*	This study[d]
YHH82	**a** *his4 trp1 ura3 bud3::TRP1 bud7-1*	This study[d]
YHH91	**a** *his4 trp1 ura3 bud3::TRP1 bud8-2*	This study[e]
YHH92	α *his4 trp1 ura3 bud3::TRP1 bud8-2*	This study[e]
YHH93	α *his4 trp1 ura3 bud3::TRP1 bud9-1*	This study[e]
YHH94	**a** *his4 trp1 ura3 bud3::TRP1 bud9-1*	This study[e]
YHH97	α *his4 trp1 ura3 bud3::TRP1 bud8-1*	This study[e]
YHH98	**a** *his4 trp1 ura3 bud3::TRP1 bud8-1*	This study[e]
YHH99	**a** *his4 trp1 ura3 bud3::TRP1 bud9-3*	This study[e]
YHH100	α *his4 trp1 ura3 bud3::TRP1 bud9-3*	This study[e]
YHH112	α *his4 trp1 ura3 bud7-1*	Segregant from YHH82 × 1237-13C
YHH113	**a** *his4 trp1 ura3 bud7-1*	Segregant from YHH82 × 1237-13C
YHH114	**a** *his4 trp1 ura3 bud9-1*	Segregant from YHH93 × 1237-1
YHH115	α *his4 trp1 ura3 bud9-1*	Segregant from YHH93 × 1237-1
YHH128	α *his4 trp1 ura3 bud3::TRP1 bud5::URA3*	Segregant from 206 × YJZ34
YHH130	α *leu2 trp1 ura3 rsr1::URA3*	Segregant from Y301 × 1237-1
YHH132	**a** *his4 trp1 ura3 bud3::TRP1 cdc24-4*	Segregant from 486 × YJZ187
YHH137	**a** *his4 trp1 ura3 bud8-1*	Segregant from YHH97 × 1237-1
YHH138	α *his4 trp1 ura3 bud8-1*	Segregant from YHH97 × 1237-1
YHH150	**a**/α *his4/his4 trp1/trp1 ura3/ura3 bud7-1/bud7-1*	YHH112 × YHH113
YHH152	**a**/α *his4/his4 trp1/trp1 ura3/ura3 bud9-1/bud9-1*	YHH114 × YHH115
YHH158	α *his4 trp1 ura3 bud3::TRP1 rsr1::URA3*	Segregant from YHH130 × YJZ34
YHH190	**a**/α *his4/his4 trp1/trp1 ura3/ura3 bud8-1/bud8-1*	YHH137 × YHH138
YHH286	α *leu2 lys2 trp1 ura3 bud2Δ::LEU2*	Segregant from HP24 × 1237-13C
YHH294	**a**/α *his4/his4 trp1/trp1 ura3/ura3 bud3::TRP1/bud3::TRP1 bud8-1/bud8-1 bud9-1/bud9-1*	Obtained by mating segregants from YHH94 × YHH97
YHH297	**a** *leu2 trp1 ura3 bud3::TRP1 bud2Δ::LEU2*	Segregant from YHH16 × YHH286
YHH301	**a**/α *his4/his4 trp1/trp1 ura3/ura3 bud3::TRP1/bud3::TRP1 bud6-1/bud6-1 bud8-1/bud8-1*	Obtained by mating segregants from YHH97 × YJZ195
YHH305	**a**/α *his4/his4 trp1/trp1 ura3/ura3 bud3::TRP1/bud3::TRP1 bud6-1/bud6-1 bud9-1/bud9-1*	Obtained by mating segregants from YHH93 × YJZ195
YHH344	**a** *ilv5 trp1* Ura$^-$ *bud3::TRP1*	Segregant from C82-1857 × 486
YHH349	α *arg4? leu1 trp1 bud3::TRP1*	Segregant from S2072A × 486
YHH354	**a** His$^-$ *trp1 ura3 msb2::URA3 bud3::TRP1*	Segregant from Y548 × YJZ34
YHH357	**a** *his4 trp1 ura3 dbf2-2 bud3::TRP1*	Segregant from L181-6B × YJZ34

Continued on following page

TABLE 1—*Continued*

Strain or plasmid	Genotype or description	Source or reference
YHH374	**a**/α *his4/his4 trp1/trp1 ura3/ura3 bud3*::*URA3*/*bud3*::*URA3 bud7-1/bud7-1*	Obtained by mating segregants from MM5.4 × YHH113
YJZ34	**a** *his4 trp1 ura3 bud3*::*TRP1*	Segregant from 486 × 1237-1
YJZ187	**a** *trp1 ura3 cdc24-4*	Segregant from Y147 × 1237-13C
YJZ193	**a** *his4 trp1 ura3 bud6-1*	Segregant from YJZ196 × 1237-1
YJZ194	α *his4 trp1 ura3 bud6-1*	Segregant from YJZ196 × 1237-1
YJZ195	**a** *his4 trp1 ura3 bud3*::*TRP1 bud6-1*	This study[e]
YJZ196	α *his4 trp1 ura3 bud3*::*TRP1 bud6-1*	This study[e]
YJZ197	α *his4 trp1 ura3 bud3*::*TRP1 spa2-10*	This study[e]
YJZ198	**a** *his4 trp1 ura3 bud3*::*TRP1 spa2-10*	This study[e]
YJZ199	**a** *his4 trp1 ura3 spa2-10*	Segregant from YJZ197 × 1237-1
YJZ200	α *his4 trp1 ura3 spa2-10*	Segregant from YJZ197 × 1237-1
YJZ203	**a** *his4 trp1 ura3 bud2-21*	Segregant from YJZ205 × 1237-1
YJZ204	α *his4 trp1 ura3 bud2-21*	Segregant from YJZ205 × 1237-1
YJZ205	α *his4 trp1 ura3 bud3*::*TRP1 bud2-21*	This study[e]
YJZ206	**a** *his4 trp1 ura3 bud3*::*TRP1 bud2-21*	This study[e]
YJZ208	**a**/α *his4/his4 trp1/trp1 ura3/ura3 bud6-1/bud6-1*	YJZ193 × YJZ194
YJZ211	**a**/α *his4/his4 trp1/trp1 ura3/ura3 bud2-21/bud2-21*	YJZ203 × YJZ204
YJZ217	**a** *his4 leu2 trp1 ura3 bud3*::*TRP1*	This study[c]
YJZ219	α *his4 trp1 ura3 bud5-4*	Segregant from YJZ220 × 1237-1
YJZ220	α *his4 trp1 ura3 bud3*::*TRP1 bud5-4*	This study[e]
YJZ223	**a**/α *his4/his4 trp1/trp1 ura3/ura3 spa2-10/spa2-10*	YJZ199 × YJZ200
YJZ244	**a** *his4 trp1 ura3 bud5*::*URA3*	Segregant from 162 (11)
YJZ256	**a** *his4 trp1 ura3 bud3*::*TRP1 bud5*::*URA3*	Segregant from YJZ244 × 486
YJZ265	**a**/α *his4/his4 trp1/trp1 ura3/ura3 bud3*::*TRP1*/*bud3*::*TRP1 bud7-1/bud7-1 bud9-1/bud9-1*	Obtained by mating segregants from YHH81 × YHH94
YJZ266	**a**/α *his4/his4 trp1/trp1 ura3/ura3 bud3*::*TRP1*/*bud3*::*TRP1 bud7-1/bud7-1 bud8-1/bud8-1*	Obtained by mating segregants from YHH82 × YHH97
YJZ271	**a** *ade2* His$^-$ *leu2 trp1 ura3 bud3*::*TRP1 bni1*::*LEU2*	Segregant from JF17 × YJZ217
YJZ280	α *his4 trp1 ura3 bud3*::*TRP1 sur4*::*URA3*	Segregant from A3-2D × 486
YJZ281	α *his4 trp1 ura3 bud3*::*TRP1 fen1*::*URA3*	Segregant from LG70-7A × 486
YJZ287	**a** *ade2* His$^-$ *lys2 trp1 ura3 bud3*::*TRP1 spa2*-Δ*3*::*URA3*	Segregant from Y601 × YJZ34
YJZ301	α *his4 leu2 trp1 ura3 bud3*::*TRP1 bni1-2*	This study[f]
YJZ302	**a** *his4 leu2 trp1 ura3 bud3*::*TRP1 bni1-2*	This study[f]
YJZ304	α *ade3 trp1 ura3 bud3*::*TRP1 cdc3-1*	Segregant from M-154 × 486
YJZ306	**a** *his4 leu2 trp1 ura3 bni1-2*	Segregant from YJZ302 × 1237-13C
YJZ307	α *his4 leu2 trp1 ura3 bni1-2*	Segregant from YJZ302 × 1237-13C
YJZ308	**a**/α *his4/his4 leu2/leu2 trp1/trp1 ura3/ura3 bni1-2/bni1-2*	YJZ306 × YJZ307
YJZ317	α *ade2 arg4*? His$^-$ *trp1* Ura$^-$ *bud3*::*TRP1 cdc25-2*	Segregant from BR205-2 × 486
YJZ319	α His$^-$ Ura$^-$ *bud3*::*TRP1 cdc31-1*	Segregant from 12021 × 486[g]
YJZ320	α *his4 ura3 bud3*::*TRP1 myo2-66*	Segregant from SLY254 × 486[g]
Plasmids		
YCp50	*CEN4 ARS1 URA3* (low copy number)	60
YEp24	*URA3* (multicopy)	9
YEp352	*URA3* (multicopy)	37
p13	*BUD3* in YCp50	13
B34	*BUD2* in YCp50	Original clone of *BUD2* (53)
pMIN1	*BUD5* in YCp50	11
p39L12	*BNI1* in YEp352	26
p183	*Sal*I-*Bam*HI fragment containing *SPA2* in YEp24	K. Madden
pJM3	*MAT***a** in YCp50	11

[a] Yeast Genetics Stock Center, Berkeley, Calif.
[b] Derived by further backcrossing of strains described by Lillie and Brown (47).
[c] A *leu2* segregant from 486 × 1241-2D was backcrossed twice more into 486.
[d] Segregant from the third backcross of the original mutant isolate to 486 and/or YJZ34.
[e] Segregant from the fourth backcross of the original mutant isolate to 486 and/or YJZ34.
[f] Segregant from a cross of YJZ217 to a segregant from the backcross of the original mutant isolate to YJZ34.
[g] The desired segregant was identified as Ts$^-$ (hence *cdc31-1* or *myo2-66*) and bipolar budding (hence *bud3*::*TRP1*). Other possible markers were not checked.

plated per 10-cm YPD plate and subjected to 40 s of UV irradiation. Surviving cells were allowed to grow in the dark at 30°C for 3 days, and individual colonies were then picked for analysis as described below.

Ethyl methanesulfonate (EMS) mutagenesis was performed as described previously (45) on stationary-phase cells of strain 486. Samples were taken at times ranging from 80 to 230 min, mixed 1:1 with 30% glycerol, and frozen at −70°C. Aliquots were thawed, and cells were plated onto YPD medium to determine survival. The 110-min sample gave ~1% survival and was used for the mutant screen. Individual colonies from YPD plates were picked for analysis as described below.

Isolation and characterization of budding-pattern mutants. Individual colonies of mutagenized cells were picked with toothpicks and suspended in 100-μl aliquots of sterile water in the wells of microtiter plates. Cells were transferred from the wells onto YPD plates by using a multiprong device to preserve each clone for further analysis. Next, 10-μl aliquots of the clonal cell suspensions were spotted onto gelatin-coated 75- by 50-mm glass microscope slides, with 28 clones

in a 7-by-4 grid on each slide. Cells were allowed to settle onto the slides for 10 min, the water was aspirated, and the slides were air dried for ≥10 min. Then 120 to 170 μl of Calcofluor solution (Sigma; 1 μg/ml in water) was placed on each slide to stain bud scars (55), and a 65- by 48-mm coverslip was applied. Slides were examined immediately or after storage overnight at 4°C by using a Nikon Microphot EPI-FL3 epifluorescence microscope with UV-2A filter set and APO 60/1.40 NA oil immersion objective. Clones that appeared to have abnormal budding patterns were recovered from the YPD plates and streaked to isolate single colonies for further analysis. The budding patterns of the mutant clones were reexamined, and clones that exhibited random budding patterns were transformed with a *BUD3*-containing plasmid to determine if the mutations affected the bipolar pattern specifically (see Results). The mutants that appeared most promising from these tests were backcrossed to strains YJZ34 and/or 486, and mutants whose phenotypes segregated cleanly were analyzed further. The mutants described in detail in this report were backcrossed two to four times (see Results and Table 1) before they were tested for complementation, linkage, and epistasis and subjected to detailed phenotypic characterization.

For detailed characterization of budding patterns and for photomicroscopy, cells were grown to mid-exponential phase in YM-P medium, fixed with formaldehyde and stained with Calcofluor as described previously (55), and examined by fluorescence microscopy as described above. The Calcofluor-stained cells or unstained cells were also examined by phase-contrast or differential interference contrast microscopy to assess overall cell morphologies. For rapid determinations of budding patterns (e.g., in scoring segregants during genetic crosses), cells from colonies or patches on solid medium were picked with a toothpick, swirled into 4 to 10 μl of 1-μg/ml aqueous Calcofluor, and examined immediately. To evaluate growth rates on solid media, cells were streaked to give single colonies on YPD or SC medium at various temperatures and the plates were checked daily to determine colony sizes. To determine growth rates in liquid medium, cells growing exponentially in YM-P medium at 30 or 37°C were diluted twofold with fresh medium at the same temperature, and the times required for the cultures to return to the original absorbance values were noted, as were the slopes of the growth curves over a period of several hours. Cultures were maintained throughout at cell densities low enough that absorbance was proportional to cell number (57). Mating abilities were tested by mixing **a** and α cells from exponentially growing cultures and collecting the cells on filters essentially as described previously (58). After incubation of the filters for 3 h on YPD plates, cells were removed by vortexing and sonicated briefly, and the numbers of zygotes were counted.

For physical mapping of genes, fragments isolated from complementing plasmids were labeled with ^{32}P by random priming (64) and hybridized to filters containing lambda clones (American Type Culture Collection, Rockville, Md.) covering most of the yeast genome (59).

RESULTS

Isolation and initial characterization of mutants. We sought to identify mutations that specifically affect the bipolar budding pattern. To allow the detection of recessive mutations, we used the haploid *bud3* deletion strain 486 (Table 1), which displays an apparently typical bipolar budding pattern (Fig. 1A) (13). To maximize the chances of obtaining the desired mutants, we performed two separate screens with mutagens (UV light and EMS) of different mutagenic specificities (33, 42, 43). The protocols used (see Materials and Methods) ensured that all mutants analyzed were of independent origin.

From 11,000 UV-mutagenized and 9,500 EMS-mutagenized clones examined, we identified 78 mutants that appeared to have reproducible alterations of budding pattern; these mutants fell into three phenotypic classes (Fig. 1B to I; Table 2). In the "random" mutants (Fig. 1B to F), bud scars appeared to be randomly distributed over the surfaces of the cells. In the "unipolar" mutants (Fig. 1H and I), almost all cells had bud scars only at the proximal pole or only at the distal pole. The "heterogeneous" mutants (Fig. 1G) displayed a complex mixture of budding patterns within a single clone, including cells with bud scars exclusively at one pole, cells with chains of bud scars reminiscent of those on axially budding cells, cells with apparently random bud scars, and cells with bud scars at both poles (like the parent strain).

It seemed likely that the random mutants would be of two types. One type would be defective in general bud site selection genes such as *RSR1*, *BUD2*, and *BUD5* (see Introduction), whereas the second type would be defective in functions necessary specifically for the bipolar budding pattern. To discriminate between these possibilities, the random mutants were transformed with the *BUD3*-containing plasmid p13 (Table 1). One of the 37 mutants could not be transformed and thus was not studied further. Of the remaining mutants, 23 continued to bud randomly in the presence of wild-type *BUD3* (data not shown), suggesting that they were defective in general bud site selection functions; these mutants will be described in more detail elsewhere. In contrast, 13 mutants displayed seemingly normal axial budding when transformed with p13 (data not shown, but compare Fig. 1K through O), suggesting that their defects were indeed specific to the bipolar pattern. As expected, these mutants all continued to bud randomly when transformed with the control plasmid YCp50.

The 13 bipolar budding-specific random mutants (see above), 12 unipolar mutants (Table 2), and 1 heterogeneous mutant with a particularly clear-cut phenotype (Fig. 1G) were selected for further analysis. Each mutant was first backcrossed to strain YJZ34 (congenic to the parental strain 486). All diploids obtained from this cross displayed seemingly normal bipolar budding (data not shown), indicating that all of the mutations are recessive. (Data presented below [Tables 4 and 5] demonstrate that **a**/α *bud3*/*bud3* diploids homozygous for the mutations described in detail here display the same budding-pattern phenotypes as the original α *bud3* haploid mutants and also confirm that the mutations are recessive in a $Bud3^-$ background. Other data presented below [Tables 4 and 5] demonstrate that each of the mutations described in detail here is also recessive when examined in a $Bud3^+$ background.)

For four of the unipolar mutants, these first-backcross diploids did not sporulate; these mutants were not studied further. For many of the other mutants, poor spore viability and poor growth of many of the viable segregants (probably because of other mutations induced by the heavy mutagenesis) made it difficult to evaluate from these first backcrosses whether the budding-pattern defects were due to single mutations. Thus, for each mutant, a segregant displaying a clear budding-pattern defect was backcrossed a second time to strain YJZ34, 486, or YJZ217. For two of the unipolar mutants and three of the random mutants, the budding-pattern defects were undetectable (or detectable only rarely) in the segregants from these second backcrosses; these mutants were not studied further. One random mutant (J14 [Table 3]) that showed a clear 2:2 segregation of the budding-pattern defect in this second backcross was studied further with segregants from this backcross.

FIG. 1. Budding patterns of parental and mutant strains. Exponentially growing cells were stained with Calcofluor and viewed by fluorescence microscopy as described in Materials and Methods. Left column (A to I), α *bud3*::*TRP1* strains (derived by several backcrosses from the original mutants, as described in the text), displaying the mutant phenotypes; middle column (J to R), α *BUD3* strains, displaying normal axial budding; right column (S to AA), **a**/α *BUD3*/*BUD3* strains, displaying the mutant phenotypes. Strains: control strains 486 (A), 1237-13C (J), and 52 (S); *bud2-21* strains YJZ205 (B), YJZ204 (K), and YJZ211 (T); *bud5-4* strains YJZ220 (C), YJZ219 (L), and YJZ219 harboring plasmid pJM3 (U); *spa2-10* strains YJZ197 (D), YJZ200 (M), and YJZ223 (V); *bni1-2* strains YJZ301 (E), YJZ307 (N), and YJZ308 (W); *bud6-1* strains YJZ196 (F), YJZ194 (O), and YJZ208 (X); *bud7-1* strains YHH81 (G), YHH112 (P), and YHH150 (Y); *bud8-1* strains YHH97 (H), YHH138 (Q), and YHH190 (Z); *bud9-1* strains YHH93 (I), YHH115 (R), and YHH152 (AA). Birth scars (arrowheads) identifying the proximal pole are easily visualized in the **a**/α *bud9-1* cells (AA) and in some of the **a**/α *bud7-1* cells (Y) but are harder to see in the **a**/α *bud8-1* cells and in other **a**/α *bud7-1* cells because of the accumulation of bud scars around the proximal pole. Comparable *bud8-2* strains were indistinguishable from the *bud8-1* strains depicted here; *bud9-2* and *bud9-3* strains were not examined in detail.

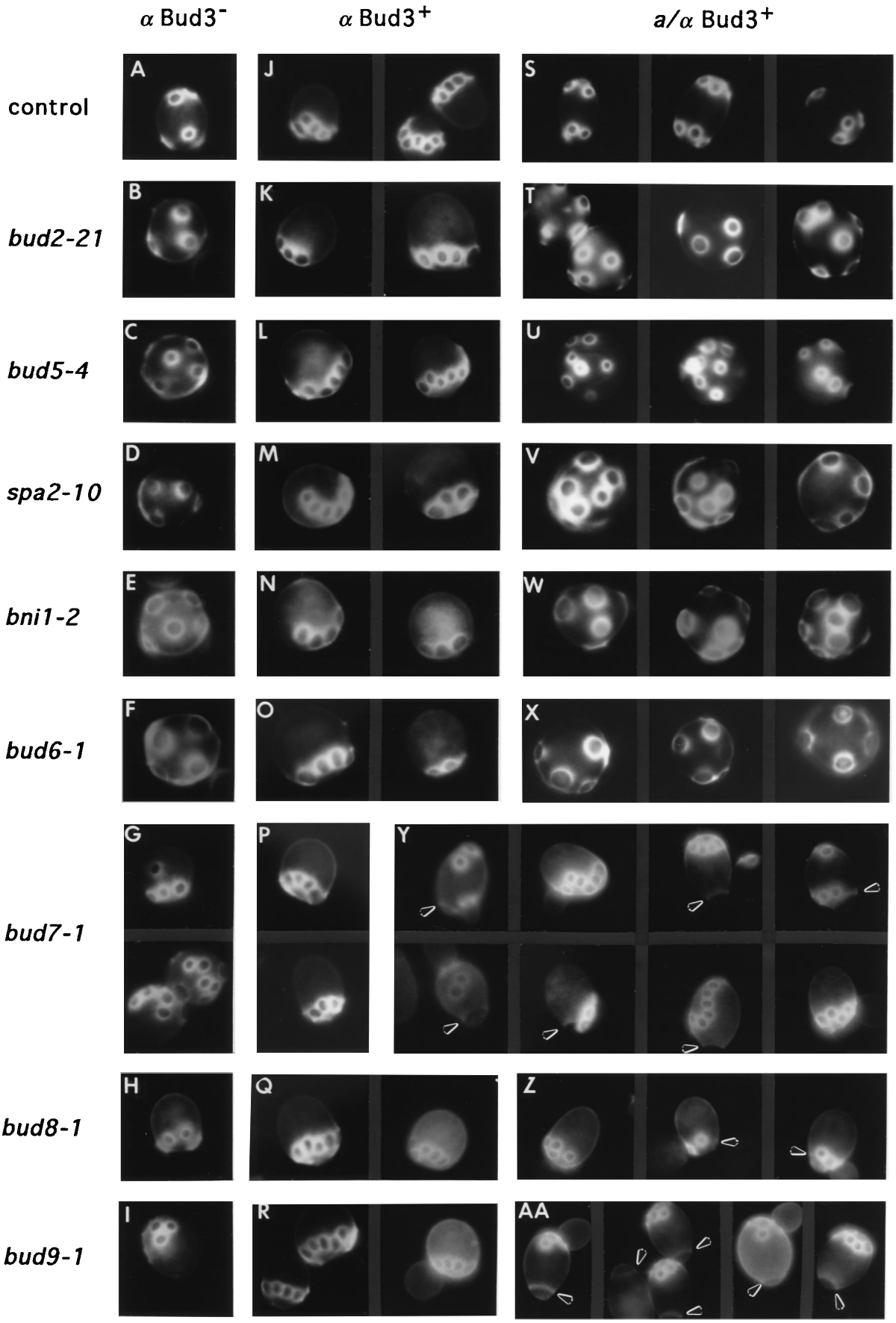
α Bud3⁻
α Bud3⁺
a/α Bud3⁺
control
bud2-21
bud5-4
spa2-10
bni1-2
bud6-1
bud7-1
bud8-1
bud9-1
A
J
S
B
K
T
C
L
U
D
M
V
E
N
W
F
O
X
G
P
Y
H
Q
Z
I
R
AA

TABLE 2. Mutants detected during the initial screen

Budding-pattern phenotype[a]	No. of independent mutants detected by:	
	UV mutagenesis (*n*/11,000)	EMS mutagenesis (*n*/9,500)
Random	13	24
Unipolar	7	5
Heterogeneous	14	15

[a] See the text and the legend to Fig. 1 for descriptions of these phenotypes.

The remaining 16 mutants were backcrossed once or twice more, starting with a segregant from the second backcross that displayed a clear budding-pattern defect. Five random mutants and one unipolar mutant showed complex segregation patterns, suggesting that two or more mutations were responsible for the original phenotype; these mutants were not studied further. The remaining 10 mutants (Table 3) showed a clear 2:2 segregation of the budding-pattern defects through at least 10 tetrads in the third and fourth backcrosses, indicating that the phenotype was due to a single mutation in each case; these mutants were studied further with segregants from the third (mutants H46 and H43) or fourth (the remaining mutants) backcross. Examination of segregants derived from the unipolar mutants revealed that the H47 and H38 derivatives budded consistently from their proximal poles, whereas the H40, H43, and H50 derivatives budded consistently from their distal poles (see the more detailed characterization below).

Genetic analyses. Complementation and linkage analyses revealed that the random mutants J36, J9, J7, and J14 contained mutations in the previously known genes *BUD2*, *BUD5*, *SPA2*, and *BNI1*, respectively (Table 4). To confirm these results, strains YJZ206 (J36), YJZ220 (J9), YJZ197 (J7), and YJZ301 (J14) were transformed with plasmids (Table 1) containing *BUD2* (B34), *BUD5* (pMIN1), *SPA2* (p183), or *BNI1* (p39L12), respectively. In each case, the transformants displayed bipolar budding (indicating complementation of the mutation of interest in the *bud3* background), whereas transformants containing the control plasmid YCp50, YEp24, or YEp352 displayed random budding like that of the untransformed strains. Henceforth, the mutations from mutants J36, J9, J7, and J14 are referred to as *bud2-21* (see references 7, 12, 19, and 53), *bud5-4* (see reference 11), *spa2-10* (see reference 69), and *bni1-2* (see reference 26).

Additional complementation and linkage analyses (Table 5) showed that the mutations in the remaining seven mutants defined four distinct genes, that the mutation from H38 is allelic to that from H47 (consistent with their similar phenotypes [see above]), and that the mutations from H43 and H50 are allelic to that from H40 (consistent with their similar phenotypes [see above]). From these results, we defined the four genes (and corresponding mutant alleles) *BUD6* (J34, *bud6-1*), *BUD7* (H46, *bud7-1*), *BUD8* (H47, *bud8-1*; H38, *bud8-2*), and *BUD9* (H40, *bud9-1*; H43, *bud9-2*; H50, *bud9-3*). Evidence that these four genes are novel came from determining their genetic map positions (Table 6; Fig. 2). These map positions distinguish *BUD6*, *BUD7*, *BUD8*, and *BUD9* from most previously described genes known to affect bud position, including *ACT1*, *AXL1*, *BNI1*, *BUD2*, *BUD3*, *BUD5*, *CDC3*, *CDC10*, *CDC11*, *CDC12*, *CDC24*, *CDC42*, *FEN1*, *RSR1*, *RVS161*, *RVS167*, and *SPA2*, all of which have been mapped to different chromosomal locations (8, 51, 63). Map positions have not been reported for two other genes affecting bud position,

TABLE 3. Summary of genetic analyses

Budding pattern	Mutant	Mutagen	Gene
Random	J36	UV	*BUD2*
	J9	EMS	*BUD5*
	J7	EMS	*SPA2*
	J14	UV	*BNI1*
	J34	UV	*BUD6*
Heterogeneous	H46	UV	*BUD7*
Unipolar (proximal pole)	H47	UV	*BUD8*
	H38	EMS	*BUD8*
Unipolar (distal pole)	H40	EMS	*BUD9*
	H43	UV	*BUD9*
	H50	UV	*BUD9*

TABLE 4. Evidence that mutants J36, J9, J7, and J14 carry mutations in *BUD2*, *BUD5*, *SPA2*, and *BNI1*, respectively[a]

Tester strain[b]	Budding pattern and segregation data for cross with mutant strain[c]:			
	J36 (YJZ205 or YJZ206)[d]	J9 (YJZ220)	J7 (YJZ197 or YJZ198)[e]	J14 (YJZ301)
J36 (YJZ206)	Random	Bipolar	Bipolar	ND
J7 (YJZ198)	ND	Bipolar	Random	ND
J14 (YJZ302)	ND	Bipolar	ND	Random
bud2-1 (124)	Random, 29:0:0	ND	ND	ND
*bud5*Δ (YJZ256 or 206)[f]	Bipolar	Random, 27:0:0	Bipolar	Bipolar
*spa2*Δ (YJZ287)	ND	Bipolar	Random, 20:0:0	ND
*bni1*Δ (YJZ271)	ND	ND	Bipolar	Random, 17:0:0

[a] Shown for each cross are the budding pattern of the diploid strain (random budding implies noncomplementation; bipolar budding implies complementation) and the results of tetrad analysis, if performed (given as number of parental ditypes:number of nonparental ditypes:number of tetratypes). The putative noncomplementation results are meaningful only if each mutation is known to be recessive. Data in this table show that the mutations from J36, J9, J7, and J14 are all recessive in a Bud3$^-$ background and that the mutations from J36 and J7 are also recessive in a Bud3$^+$ background; the latter point was established also for the mutations from J9 and J14 by the observation that the diploids formed by mating YJZ220 to 1237-1 and YJZ302 to 1237-13C both budded bipolarly. Data in the table also show that the *spa2*Δ and *bni1*Δ mutations are recessive in a Bud3$^-$ background (as required for the interpretation of the noncomplementation results shown here) and that the *bud5*Δ mutation is recessive in both Bud3$^+$ and Bud3$^-$ backgrounds (see also reference 11). *bud2-1* was shown previously to be recessive with respect to its effect on axial budding (12); the recessiveness of *bud2-1* with respect to its effect on bipolar budding was confirmed by the observation that the diploid formed by mating strains 124 and 1237-1 budded bipolarly. The tetrad analyses of *bud5*Δ × J9, *spa2*Δ × J7, and *bni1*Δ × J14 were straightforward to interpret because each diploid was homozygous for *bud3*::*TRP1*. Thus, every tetrad yielded four random-budding segregants, showing the tight linkage of the new budding-pattern mutation to the tester mutation. The tetrad analysis of *bud2-1* × J36 was more complex because this diploid was heterozygous, *BUD3*/*bud3*::*TRP1*. Of the 29 tetrads analyzed, 2 yielded four random-budding segregants (presumably 2 *bud2-1 BUD3*:2 *J36 bud3*) and 27 yielded three random-budding segregants plus one axial-budding segregant. If *bud2-1* and mutation *J36* are in fact allelic and therefore tightly linked, these 27 tetrads would presumably represent a segregation of 1 *bud2-1 BUD3* (random):1 *bud2-1 bud3* (random):1 *J36 bud3* (random):1 *J36 BUD3* (axial). To confirm that the axially budding segregants were indeed all *J36 BUD3*, each such segregant was mated to another axially budding segregant (from the same cross) of opposite mating type. As expected, each resulting diploid displayed random budding. ND, cross not performed.

[b] Strains 124 and 206 are *BUD3*; the other tester strains are *bud3*::*TRP1*.

[c] All strains are *bud3*::*TRP1*.

[d] YJZ205 was used for the cross to the J36 tester; YJZ206 was used for the other crosses.

[e] YJZ198 was used for the cross to the *bud5*Δ tester; YJZ197 was used for the other crosses.

[f] YJZ256 was used for the crosses to the J9 and J14 testers; 206 was used for the other crosses.

TABLE 5. Complementation and linkage analyses among the novel mutants[a]

Mutant strain[b]	Budding pattern and segregation data for cross with mutant strain[c]:				
	J34 (YJZ196)	H46 (YHH81)	H47 (YHH97)	H40 (YHH93)	H50 (YHH100)
J34 (YJZ195)	Random	Bipolar, 3:5:8	Bipolar, 5:0:11	Bipolar, 0:3:11	ND[d]
H46 (YHH82)	ND	Heterogeneous	Bipolar, 3:1:6	ND	Bipolar
H47 (YHH98)	ND	ND	Unipolar	ND	Bipolar
H38 (YHH91)	ND	Bipolar, 3:4:6	Unipolar, 20:0:0	Bipolar, 2:3:7	Bipolar
H40 (YHH94)	ND	Bipolar, 2:2:7	Bipolar, 1:2:7	Unipolar	Unipolar
H43 (YHH76)	ND	Bipolar	Bipolar	Unipolar,[e] 20:0:0[e]	Unipolar, 20:0:0

[a] Shown for each cross are the budding pattern of the diploid strain (bipolar budding implies complementation, aberrant budding [random, heterogeneous, or unipolar] implies noncomplementation) and the results of tetrad analysis, if performed (given as number of parental ditypes:number of nonparental ditypes:number of tetratypes). The putative noncomplementation results are meaningful only if each mutation is known to be recessive. Data in this table establish that each mutation is recessive in a Bud3$^-$ background. That each mutation is also recessive in a Bud3$^+$ background was established by crossing strains YJZ196, YHH82, YHH97, YHH92, YHH93, YHH77, and YHH100 to 1237-1 or 1237-13C; each resulting diploid displayed bipolar budding. As all of the diploids analyzed here were homozygous *bud3*/*bud3*, the tetrad data were straightforward to interpret; parental ditypes had all four segregants with aberrant budding patterns (random, heterogeneous, or unipolar), nonparental ditypes had two aberrantly budding segregants and two bipolar-budding segregants, and tetratypes had three aberrantly budding segregants and one bipolar-budding segregant. Not shown is that **a**/α *bud3*/*bud3* diploids homozygous for the mutations from H38 (YHH91 × YHH92), H43 (YHH76 × YHH77), and H50 (YHH99 × YHH100) also displayed unipolar budding.

[b] All strains are **a** *bud3*::*TRP1*.

[c] All strains are α *bud3*::*TRP1*.

[d] ND, cross was not performed.

[e] These data are actually from the reciprocal cross of YHH77 × YHH94.

BUD4 (12) and *SUR4* (25). Complementation and linkage analyses showed that *BUD6*, *BUD7*, *BUD8*, and *BUD9* were distinct from these genes (Table 7).

Characterization of mutant budding-pattern phenotypes. The analyses described above suggested that a mutation in any of eight genes could give rise to bipolar budding-specific defects in the budding pattern (Table 3). To characterize the mutant phenotypes in more detail, we first constructed **a**, α, and **a**/α strains carrying the new mutations (except for *bud9-2* and *bud9-3*) in a *BUD3* background. To this end, backcrossed strains carrying the new mutations in the *bud3*::*TRP1* background were crossed to a congenic *BUD3* strain (1237-1 or 1237-13C). Each cross yielded apparent nonparental ditype tetrads (2 bipolar-budding Trp$^+$:2 axially budding Trp$^-$), apparent tetratype tetrads (1 bipolar-budding Trp$^+$:1 aberrant-budding Trp$^+$:2 axially budding Trp$^-$), or both, for the new mutation and *bud3*::*TRP1*. To confirm that all of the axially budding Trp$^-$ segregants from the presumed nonparental ditypes and half of those from the presumed tetratypes indeed carried the new mutations in a *BUD3* background, two approaches were used. In some cases, the strains to be tested were crossed to tester strains carrying the same new mutation in a *bud3*::*TRP1* background (for *bud5-4*, the *bud3*::*TRP1 bud5*::*URA3* strain YJZ256 was used as a *MAT***a** tester); for a strain carrying the new mutation, both the resulting diploid and all of the Trp$^+$ segregants from that diploid should display the appropriate aberrant budding pattern. In other cases, the strains to be tested were crossed to tester strains (486 and YJZ34) carrying only the *bud3*::*TRP1* mutation; for a strain carrying the new mutation, all of the resulting diploids should display normal bipolar budding, but ~50% of their Trp$^+$ segregants should display the appropriate aberrant budding pattern. In all cases, the results confirmed the original identification of nonparental ditype and tetratype tetrads. Sibling **a** and α clones that were known to carry the new mutations in a

TABLE 6. Linkage data for *BUD6*, *BUD7*, *BUD8*, and *BUD9*[a]

Cross	Marker pair	No. of tetrads			Map distance (cM)[b]
		PD	NPD	T	
YJZ195 × YJZ304	*bud6 cdc3*	16	0	2	6
YJZ195 × YJZ317	*bud6 cdc25*	11	0	3	11
YHH82 × YJZ320	*bud7 myo2*	16	0	4	10
YHH82 × YJZ319	*bud7 cdc31*	10	0	6	19
YHH97 × YJZ195	*bud8 bud6*	5	0	11	34
YHH97 × YHH344	*bud8 ilv5*	19	0	3	7
YHH94 × YHH349	*bud9 leu1*	16	0	4	10
YHH93 × YHH354	*bud9 msb2*	18	0	2	5
YHH93 × YHH357	*bud9 dbf2*	11	1	12	37

[a] All crosses were homozygous *bud3*::*TRP1*/*bud3*::*TRP1*, so that each cross except for YHH97 × YJZ195 (*bud8* × *bud6*) segregated 2 bipolar (*BUDX bud3*): 2 nonbipolar (*budX bud3*). The *cdc3*, *cdc25*, *myo2*, *cdc31*, and *dbf2* markers were scored by their Ts$^-$ phenotypes, whereas the *ilv5*, *leu1*, and *msb2*::*URA3* markers were scored on appropriate selective media. In the *bud8* × *bud6* cross, two types of tetrads were observed. Segregation of 2 unipolar (presumably *bud8 BUD6 bud3*):2 random (presumably *BUD8 bud6 bud3*) was scored as parental ditype, whereas segregation of 1 unipolar (presumably *bud8 BUD6 bud3*):2 random (presumably *BUD8 bud6 bud3* and *bud8 bud6 bud3*):1 bipolar (presumably *BUD8 BUD6 bud3*) was scored as tetratype. (Note that *bud6* is epistatic to *bud8*, as shown below.) Because the numbers of tetrads are small, map distances, calculated from Perkins's formula $X_p = 50(6\text{NPD} + \text{T})/(\text{PD} + \text{NPD} + \text{T})$, are rough estimates only. PD, parental ditype; NPD, nonparental ditype; T, tetratype.

[b] cM, centimorgans.

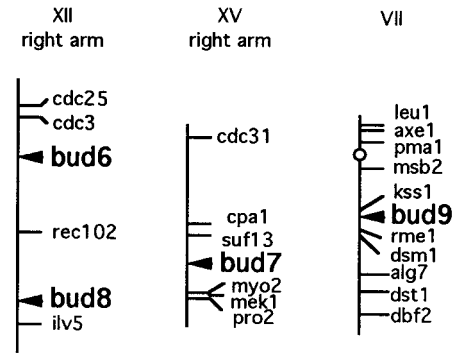

FIG. 2. Map locations of *BUD6*, *BUD7*, *BUD8*, and *BUD9* based on the genetic data in Table 6 and physical mapping of the respective cloned genes (to be described in detail elsewhere). DNA from the *bud6*-complementing plasmid hybridized to λ′ clones 3681 and 3929 (ATCC 70204 and 70235, respectively), DNA from the *bud7*-complementing clone hybridized to λ′ clones 3455 and 2128 (ATCC 70173 and 70039, respectively), DNA from the *bud8*-complementing plasmid hybridized to λ′ clone 3079 (ATCC 70109), and DNA from the *bud9*-complementing plasmid hybridized to λ′ clones 2800 and 6244 (ATCC 70083 and 70702, respectively).

TABLE 7. Evidence that *BUD6*, *BUD7*, *BUD8*, and *BUD9* are distinct from *BUD4* or *SUR4*[a]

Tester strain	Budding pattern and segregation data for cross with mutant strain[b]:			
	bud6-1 (YJZ194 or YJZ195)	*bud7-1* (YHH112 or YHH82)	*bud8-1* (YHH138 or YHH98)	*bud9-1* (YHH115 or YHH94)
bud4-1 BUD3 (191)	Bipolar, 5/5	Bipolar, 9/10	Bipolar, 9/10	Bipolar, 9/10
sur4 bud3::*TRP1* (YJZ280)	Bipolar, 5:0:5	Bipolar, 5:1:2	Bipolar, 4:0:6	Bipolar, 2:2:5

[a] Shown for each cross are the budding pattern of the diploid strain and the results of tetrad analysis of that strain. Bipolar budding indicates complementation, except perhaps for the crosses with *bud4*, for which the phenotype of a potential noncomplementing diploid is difficult to predict. For the crosses with *bud4* (diploids homozygous for *BUD3*), the tetrad data are presented as the number of tetrads containing ≥1 segregant with an aberrant budding pattern (random, heterogeneous, or unipolar)/the number of tetrads examined. Because the *bud6-1*, *bud7-1*, *bud8-1*, and *bud9-1* mutations do not affect the axial budding of **a** or α *BUD3* cells and a *bud4-1 BUD3* strain buds in a bipolar pattern (12), the aberrantly budding segregants must carry both *bud4* and the new mutation and thus indicate recombination between *bud4* and the mutation of interest. For the crosses with *sur4* (diploids homozygous for *bud3*::*TRP1*), the tetrad data are presented as number of parental ditypes (PD):number of nonparental ditypes (NPD):number of tetratypes (T), where segregations of 0 bipolar:4 aberrant budding pattern, 2 bipolar:2 aberrant budding pattern, and 1 bipolar:3 aberrant budding pattern are taken as PD, NPD, and T, respectively.

[b] The crosses to 191 used the *BUD3* strains YJZ194, YHH112, YHH138, and YHH115; the crosses to YJZ280 used the *bud3*::*TRP1* strains YJZ195, YHH82, YHH98, and YHH94.

BUD3 background were then mated to generate **a**/α *BUD3*/*BUD3* diploid strains that were homozygous for the new mutations. Because of the tight linkage of *BUD5* and *MAT* (11), we recovered no *MAT***a** *BUD3 bud5-4* segregants. Thus, the possible effect of *bud5-4* on axial budding was examined only in *MAT*α strains, and the phenotype of *bud5-4* in an **a**/α Bud3$^+$ background was examined by introducing a plasmid containing *MAT***a** (pJM3) into the α *BUD3 bud5-4* strain YJZ219.

Both **a** and α haploid strains carrying the mutations of interest in a *BUD3* background appeared to display essentially normal axial budding (Fig. 1J to R and data not shown). In contrast, the **a**/α Bud3$^+$ strains homozygous or (for *bud5-4*) hemizygous for the mutations of interest displayed aberrant budding patterns that were identical (in all cases but *bud7-1*) or similar (*bud7-1* [see below]) to those seen in the **a** or α *bud3* strains (Fig. 1T to AA; cf. Fig. 1B to I). In addition, these budding patterns were indistinguishable (except in the case of *bud7-1*) from those seen in **a**/α *bud3*/*bud3* strains (cells not shown, but see descriptions in Tables 4 and 5 and further discussion below of *bud7-1*) and in **a** or α *bud4* strains (cells not shown, but see descriptions in Table 7). Thus, each of the new mutations indeed appears to affect the bipolar budding pattern specifically.

As null alleles of *BUD2* and *BUD5* affect both the axial and bipolar budding patterns (11, 53), the *bud2-21* and *bud5-4* alleles presumably encode proteins that retain function for axial budding although not for bipolar budding (see Discussion). The same might be true of the other mutations identified here. However, null alleles of *BNI1* have been shown to affect bipolar but not axial budding (26). Moreover, we observed that **a** and α strains carrying null alleles of *SPA2* (Y601 and Y609) displayed normal or nearly normal axial budding, whereas the **a**/α diploid formed by mating these strains (Y650) appeared to bud randomly like the **a**/α *spa2-10*/*spa2-10* diploid shown in Fig. 1V (data not shown; also see below).

For the "random" mutants, it was important to determine whether bud site selection was truly random throughout the life of each cell. Accordingly, the **a**/α Bud3$^+$ strains homozygous or (for *bud5-4*) hemizygous for the mutations of interest were stained with Calcofluor under conditions that allowed visualization of the birth scars and thus unambiguous recognition of the proximal and distal cell poles. (For the genes other than *BUD2* and *BUD5*, it seemed most informative to perform this analysis on strains carrying null mutations, when possible. Thus, we used strains carrying deletion alleles of *SPA2* and *BNI1* rather than the alleles identified in this study.) We then scored the positions of bud sites on cells with zero, one, or two previous bud scars. As described previously (15), the wild-type strain budded exclusively from the two poles with a strong initial bias for use of the distal pole that disappeared in later cell cycles (Fig. 3). The *bni1*Δ and *bud5-4* cells appeared to choose bud sites essentially randomly from the first cycle onward (Fig. 3). However, remarkably, the *spa2*Δ and *bud6-1* cells (and to a lesser extent the *bud2-21* cells) appeared to choose first bud sites almost normally at the distal pole but then became progressively more random in the selection of subsequent budding sites (Fig. 3). It did appear that the first bud sites were less often precisely at the tip of the distal pole than in wild-type strains (data not shown) (see reference 15). In addition, it was striking that although the *spa2*Δ, *bud6-1*, and *bud2-21* cells often had both of their first two bud sites at the distal pole, these sites were generally not directly adjacent to each other, in contrast to the situation in wild-type cells (data not shown) (see reference 15).

Analysis of the "heterogeneous" mutant *bud7-1* revealed a number of intriguing features. Cells of an **a**/α *bud7-1*/*bud7-1* Bud3$^-$ strain (YHH374) displayed very heterogeneous budding patterns like those of the original α *bud7-1 bud3*::*TRP1* mutant; chains of bud scars, when observed, were almost always short (data not shown, but cf. Fig. 1G). The presence of the short chains of bud sites did not appear to reflect possible residual Bud3p activity in the *bud3*::*TRP1* strains (13), because strains carrying the more complete *bud3*::*URA3* deletion appeared similar (data not shown). In contrast, although **a**/α *bud7-1*/*bud7-1* Bud3$^+$ cells also displayed heterogeneous budding patterns (Fig. 1Y), many cells had longer chains of bud scars very similar to those seen on axially budding cells (Fig. 1Y; cf. Fig. 1J to R) (see reference 15). However, in contrast to normal axially budding cells, the **a**/α *bud7-1*/*bud7-1* Bud3$^+$ cells could produce chains of bud sites starting at the distal pole or in the equatorial region, as well as at the proximal pole (Fig. 1Y). Another remarkable feature of the budding patterns of the **a**/α *bud7-1*/*bud7-1* cells (more conspicuous in the Bud3$^-$ cells, but also apparently detectable in the Bud3$^+$ cells) was a bias for use of the proximal pole for the first bud site followed by a bias for use of the distal pole for the second bud site (Fig. 3).

To assess the consistency of unipolar budding in the *bud8-1* and *bud9-1* mutants, we performed similar quantitative analyses of the budding patterns of **a**/α Bud3$^+$ strains homozygous for these mutations. In contrast to the wild-type control strain (Fig. 4, top; see also Fig. 3), the *bud8* mutant budded almost exclusively from the proximal pole (Fig. 4) and the *bud9* mutant budded almost exclusively from the distal pole (Fig. 4). Observations on cells with four bud scars were particularly striking. In the wild-type strain, ~19% of such cells had all four

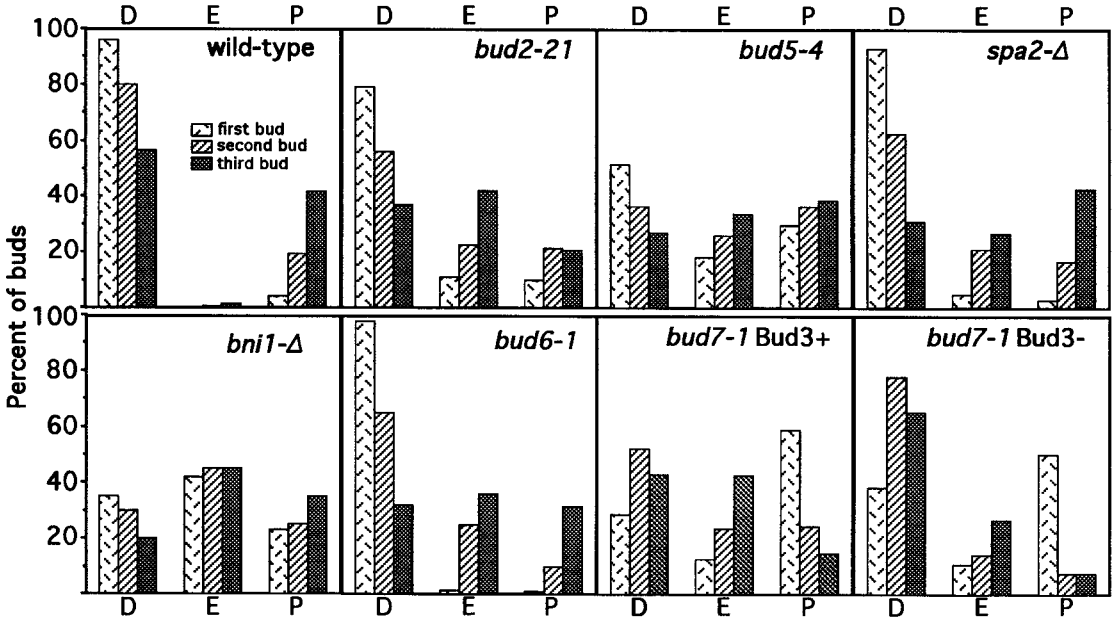

FIG. 3. Quantitative evaluation of bud position in the "random" and "heterogeneous" mutants. Exponentially growing **a**/α Bud3$^+$ cells homozygous (or hemizygous) for the mutations of interest were examined after being stained with Calcofluor; for *bud7-1*, a Bud3$^-$ strain was also examined. The positions of first bud sites (position of the bud on a budded cell with no bud scars or position of the bud scar on a cell with one bud scar), second bud sites (position of the bud on a budded cell with one bud scar), and third bud sites (position of the bud on a budded cell with two bud scars) were scored as distal pole (D; the third of the cell most distal to the birth scar), equatorial (E; the middle third of the cell), or proximal pole (P; the third of the cell centered on the birth scar). Strains used and numbers of first, second, and third bud sites scored are as follows: wild-type (strain 52), 200, 200, 200; *bud2-21* (YJZ211), 130, 130, 130; *bud5-4* (YJZ219 containing plasmid pJM3), 130, 95, 85; *spa2*-Δ (Y650), 106, 109, 101; *bni1*-Δ (JF23), 100, 100, 100; *bud6-1* (YJZ208), 230, 230, 230; *bud7-1* Bud3$^+$ (YHH150), 200, 200, 200; and *bud7-1* Bud3$^-$ (YHH374), 200, 200, 200. About 10% of the YJZ219 cells had lost plasmid pJM3, as judged by their Ura$^-$ phenotype; thus, some of the bud positions scored as proximal pole in this strain would have resulted from axial budding after loss of the *MAT***a** plasmid.

scars at the distal pole, and no cells that had all four scars at the proximal pole were detected. In contrast, ~96% of the *bud9* cells with four bud scars had all four scars at the distal pole, whereas ~78% of the *bud8* cells with four bud scars had all four scars at the proximal pole.

For the *bud8* and *bud9* mutants, it was also important to determine whether the "unipolar" budding patterns might in fact be axial budding patterns at one or the other cell pole. In exponentially growing, axially budding cells, the bud scars form a continuous chain in which each scar is directly adjacent to the immediately preceding scar (15). In contrast, bipolar-budding cells display clusters of bud scars around the cell poles that do not always form continuous chains (15). For both the *bud8* and *bud9* mutants, it was clear that the groups of bud scars resembled the clusters seen at the corresponding poles of bipolar-budding cells rather than the continuous chains seen on axially budding cells (compare Fig. 1H, I, Z, and AA to Fig. 1J through R).

Characterization of other mutant phenotypes. The mutations described here all affect the bipolar but not the axial budding pattern. However, it is possible that the genes identified by such mutations are not dedicated to specifying the bipolar budding pattern but instead also have other roles in cell growth and/or morphogenesis. As a first step in evaluating this possibility, we examined other aspects of the mutant phenotypes associated with the newly identified genes. (The functions of *BUD2*, *BUD5*, *SPA2*, and *BNI1* have been explored in detail elsewhere; see Discussion.)

First, the growth rates of **a**/α Bud3$^+$ strains homozygous for the mutations of interest (*bud6-1*, YJZ208; *bud7-1*, YHH150; *bud8-1*, YHH190; and *bud9-1*, YHH152) were compared with that of the control strain 52 (see Materials and Methods). No significant differences in growth rate were seen during growth in YM-P liquid medium at 30 or 37°C or on YPD or SC solid medium at 18, 23, or 30°C, and the *bud6-1* strain also grew as well as the control strain on solid media at 37°C. However, the *bud7-1*, *bud8-1*, and *bud9-1* strains all grew significantly more slowly than the control strain on solid media at 37°C. Cells from the liquid cultures were examined by phase-contrast or differential interference contrast microscopy, as well as by fluorescence microscopy after being stained with Calcofluor, to determine overall cell morphologies. The *bud7-1*, *bud8-1*, and *bud9-1* strains all displayed the ellipsoidal cell shape characteristic of normal **a**/α cells (Fig. 1Y to AA; cf. Fig. 1S). In contrast, the *bud6-1* cells were rounder than normal (Fig. 1X), a property that they shared with cells of the other random-budding mutants (Fig. 1T to W). In addition, the bud scars on the *bud6-1* cells were conspicuously larger than normal (Fig. 1X), in agreement with the observation that the mother bud necks of budded cells were thicker than normal (data not shown); both of these properties were also shared with the *spa2* and *bni1* mutants (Fig. 1V and W and data not shown) (also see reference 26).

Finally, mating efficiencies were evaluated by determining the numbers of zygotes produced in crosses between **a** and α *BUD3* strains carrying the mutations of interest (see Materials and Methods). *bud7-1* (YHH112 × YHH113) and *bud9-1* (YHH114 × YHH115) strains produced as many zygotes as did the control strains (1237-1 × 1237-13C). *bud6-1* (YJZ193 × YJZ194) and *bud8-1* (YHH137 × YHH138) strains also mated well, although the frequencies of zygotes observed were ~40% lower than in the control cross.

Epistasis tests. To gain insights into the functional relationships among the gene products involved in bipolar bud site

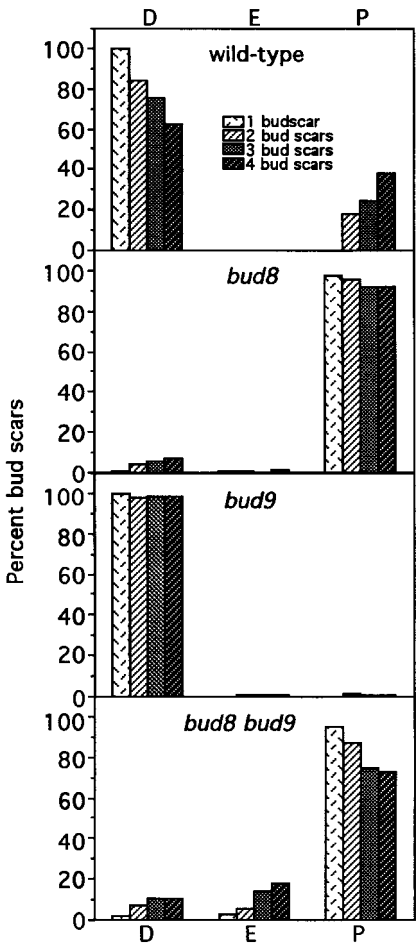

FIG. 4. Quantitative evaluation of bud position in the unipolar mutants and in the *bud8 bud9* double mutant. Exponentially growing **a**/α Bud3$^+$ cells homozygous for the mutations of interest were examined after staining with Calcofluor. The positions of all bud scars were determined on 100 cells with one bud scar, 100 cells with two bud scars, 100 cells with three bud scars, and 100 cells with four bud scars. The average values from three independent experiments are shown. Bud scar positions were defined as in Fig. 3. Strains: wild type, strain 52; *bud8-1*, YHH190; *bud9-1*, YHH152; *bud8-1 bud9-1*, YHH294.

selection, we performed epistasis tests between pairs of mutations whose phenotypes were distinct. To allow the epistasis relationships to be evaluated in haploid strains, the strains used all carried *bud3*::*TRP1*. However, in some cases, the small size of the haploid cells made it difficult to determine their budding patterns unambiguously. In these cases, diploid strains homozygous for the mutations being tested were constructed by mating appropriate pairs of haploid strains. In some cases (double mutants of *bud8* or *bud9* with *rvs161* or *rvs167*; double mutants of *bud7* with any of the mutations causing random budding), we were not able to score the budding patterns unambiguously even in diploid strains.

The results of the epistasis tests that could be scored unambiguously are shown in Table 8 and Figures 4 and 5. Each mutation causing a random or heterogeneous budding pattern was epistatic to the mutations causing unipolar budding patterns. Interestingly, the *bud6-1 bud9-1* strain resembled the *bud6-1* single mutant in that first bud sites were nearly always (96 of 100 cells scored [cf. Fig. 3]) at the distal pole, with bud position then becoming more random in subsequent cell cycles. In contrast, the *bud6-1 bud8-1* strain appeared to choose bud sites essentially randomly even in the first cell cycle; of 130 cells scored as in Fig. 3, 30 had first bud sites at the distal pole, 49 had first bud sites at the proximal pole, and 51 had first bud sites in the equatorial region. In addition, the *bud8-1* mutation (unipolar, proximal pole) was epistatic to the *bud9-1* mutation (unipolar, distal pole): the double mutant budded predominantly from its proximal pole (Fig. 4 and 5) in a pattern closely resembling (although less tight than) that of the *bud8-1* single mutant (cf. Fig. 1Z and 4).

DISCUSSION

In previous studies, genes involved in bud site selection have been identified either serendipitously (2, 4, 11, 23, 25–27, 40, 67–70) or in purposeful screens (12, 29). In many cases, it is known (or strongly suggested by the presence of pleiotropic mutant phenotypes) that these genes have roles in addition to their involvement in bud site selection (1, 2, 18, 20, 23, 25–27, 30, 40, 44, 67–70). Of the five previously known genes that appear to function exclusively in bud site selection, three are required for both the axial and bipolar budding patterns and thus define a class of general site selection functions, which include a GTPase (Rsr1p) and its regulatory factors (Bud2p and Bud5p) (see Introduction). In contrast, *BUD3* and *BUD4* are required only for axial budding and thus define a class of axial budding-specific functions, which include components (such as Bud3p and Bud4p) of the transient positional signal that marks the preceding division site on mother and daughter cells (see Introduction). Although genes required only for bi-

TABLE 8. Epistasis tests among mutations affecting the bipolar budding pattern[a]

First mutation	Budding pattern of double mutant with second mutation:	
	bud8-1 (unipolar, proximal)	*bud9-1* (unipolar, distal)
*spa2*Δ (random)	Random	Random
*bni1*Δ (random)	Random	Random
bud6-1 (random)	Random[b]	Random[b]
bud7-1 (heterogeneous)	Heterogeneous[b]	Heterogeneous[b]
bud8-1 (unipolar, proximal)		Unipolar, proximal[c]
*rsr1*Δ (random)	Random	Random
*bud2*Δ (random)	Random	Random
*bud5*Δ (random)	Random	Random
*sur4*Δ (random)	Random	Random
*fen1*Δ (random)	Random	Random
cdc24-4 (random)	Random	Random

[a] The double mutants tested for epistasis (all in a *bud3*::*TRP1* background) were recovered from the crosses described in Table 5 or from similar crosses involving the same *bud8-1* and *bud9-1* testers and strains YJZ287 (*spa2*Δ), YJZ271 (*bni1*Δ), YHH158 (*rsr1*Δ), YHH297 (*bud2*Δ), YHH128 (*bud5*Δ), YJZ280 (*sur4*Δ), YJZ281 (*fen1*Δ), and YHH132 (*cdc24-4*). Presumptive double-mutant segregants were isolated from nonparental ditype (2 bipolar budding:2 aberrant budding) or tetratype (1 bipolar budding:3 aberrant budding) tetrads, and the presence of both mutations was confirmed in either or both of two ways. First, the diploids obtained by crossing the candidate strains to each of the single-mutant parents were shown to have the expected aberrant budding phenotypes. Second, the candidate strains were crossed to testers that were wild type (except for the presence of *bud3*::*TRP1*) and the presence of both of the expected aberrant budding patterns was demonstrated among the haploid segregants. Shown in the table are the budding patterns of the double mutants as observed in the haploid *bud3* strains (double mutants involving *bni1*, *rsr1*, *bud2*, *bud5*, *sur4*, *fen1*, and *cdc24*) or in homozygous diploid strains constructed by mating appropriate pairs of these haploid strains (the remaining cases).

[b] See Fig. 5. As described in the text, detailed examination revealed that the *bud6-1 bud8-1* and *bud6-1 bud9-1* strains differed in the positioning of first bud sites on daughter cells.

[c] See Fig. 4 and 5.

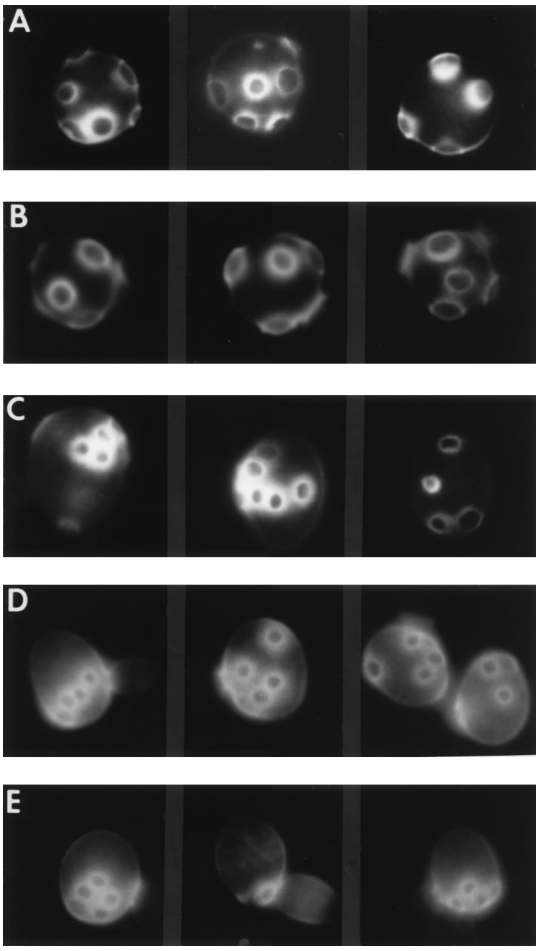

FIG. 5. Results of epistasis experiments. Exponentially growing cells were stained with Calcofluor and viewed by fluorescence microscopy as described in Materials and Methods. Cells shown are from **a**/α *bud3*::*TRP1*/*bud3*::*TRP1* diploid strains homozygous for the indicated pairs of mutations: (A) *bud6-1* and *bud8-1* (strain YHH301); (B) *bud6-1* and *bud9-1* (strain YHH305); (C) *bud7-1* and *bud8-1* (strain YJZ266); (D) *bud7-1* and *bud9-1* (strain YJZ265); (E) *bud8-1* and *bud9-1* (strain YHH294).

polar budding had not been identified, the only purposeful screens for budding-pattern mutants had used axially budding strains (12, 29), in which mutations in such genes could not have been detected. Indeed, the existence of bipolar budding-specific functions was strongly suggested by the evidence that the bipolar pattern utilizes positional signals that are distinct from the transient positional signal used in axial budding (15). In particular, the bipolar pattern appears to depend on persistent signals that mark the region of the division site and the tip of the distal pole on a newborn daughter cell, as well as each previously used division site on a mother cell (Fig. 6) (15). These observations have suggested a model in which the general site selection functions can respond either to axial budding-specific or to bipolar budding-specific positional signals (15, 56).

The studies reported here were undertaken in an attempt to identify the postulated bipolar budding-specific functions, which might include components of the persistent positional signals and/or proteins involved in positioning or responding to these signals. By screening for mutants in a bipolar-budding haploid strain, we were able to detect recessive mutations that affected the bipolar pattern. By screening individual mutagenized clones by fluorescence microscopy after staining with Calcofluor, we were able to detect a variety of alterations in the bipolar pattern. One class of mutants harbored mutations that randomized the budding pattern both in the original Bud3$^-$ parent strain and in a Bud3$^+$ derivative. Thus, these mutations presumably lie in *RSR1*, *BUD2*, *BUD5*, or genes encoding novel general site selection functions. Further analysis of these mutants is in progress.

In addition, we detected mutations in eight genes that disrupted bipolar budding but had no obvious effect on axial budding. Each mutation produced a characteristic phenotype in all genetic backgrounds in which bipolar budding would otherwise be seen, namely, **a** and α Bud3$^-$ haploids, **a** and α Bud4$^-$ haploids, and **a**/α diploids that were either Bud3$^+$ or Bud3$^-$. The observation that **a**/α Bud3$^+$ strains carrying the new mutations (except perhaps for *bud7-1* [see below]) displayed aberrant budding patterns, rather than budding axially, is noteworthy. This behavior contrasts sharply with that of **a** or α cells that lose factors necessary for axial budding either by mutation of *BUD3* or *BUD4* or because of physiological perturbations; rather than budding randomly, such cells appear to choose bud sites by using bipolar signals that are expressed in **a** and α cells but not used as long as the factors necessary for axial budding are in place (12, 13, 15, 50). As Bud3p and Bud4p also appear to be expressed and localized similarly in all cell types (13, 65), the behavior of **a**/α Bud3$^+$ Bud4$^+$ cells carrying the bipolar budding-specific mutations suggests that some other factor necessary for axial budding is absent in such cells, probably as a result of repression by the repressor **a**1/α2 (12); Axl1p appears to be at least one such factor (29). In this context, the ability of **a**/α *bud7-1*/*bud7-1* strains to form axial-like chains of bud sites, apparently in a Bud3p-dependent manner, is surprising and intriguing, especially as these chains do not always start at the proximal pole as they would during normal axial budding. At present, we cannot explain this behavior.

Of the eight genes identified in this study, four were known previously. The identification of bipolar budding-specific alleles of the general site selection genes *BUD2* and *BUD5* appears to support the model described above. Genetic and biochemical evidence indicates that the GTP-bound form of Rsr1p interacts with Cdc24p (and thus directs polarity establishment functions to the appropriate site) and that Rsr1p function requires cycling between the GTP-bound and GDP-bound forms (3, 52, 53, 62, 74). It seems likely that the localized regulation of the Rsr1p GTPase cycle would be achieved by interaction of its regulatory factors with the axial budding-specific and bipolar budding-specific positional signals. Presumably, the *bud2-21* and *bud5-4* alleles encode proteins that retain the ability to interact with the Bud3p/Bud4p-containing axial signal but have lost the ability to interact with the bipolar budding-specific positional signals. We anticipate that it should also be possible to identify alleles of *BUD2* and *BUD5* that disrupt the axial budding pattern but have no effect on the bipolar pattern; analysis of axial budding-specific and bipolar budding-specific alleles should then allow mapping of the domains through which Bud2p and Bud5p interact with the respective positional signals.

The other two previously known genes identified in this study, *SPA2* and *BNI1*, appear to function also in other aspects of polarity establishment and morphogenesis. In particular, Spa2p is required for polarized-projection (shmoo) formation in response to mating pheromone (30). The function of Spa2p during vegetative growth has been harder to define, because *spa2* null mutants grow at rates similar to that of the wild type and are not conspicuously abnormal in morphology (30, 69).

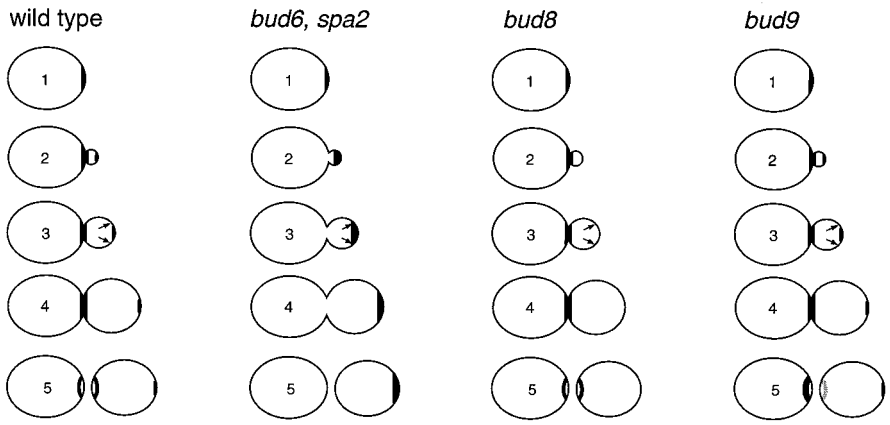

FIG. 6. Phenotypes of the *bud6*, *spa2*, *bud8*, and *bud9* mutants interpreted in terms of a model developed previously (15) for how the bipolar signal molecules might become positioned during the cell cycle. The model postulates that in wild-type cells, bipolar signal molecules accumulate at the presumptive bud site (cell 1) and are partitioned between the tip of the bud and the mother bud neck at bud emergence (cell 2); the latter signal molecules are then further partitioned between mother and daughter cells at cell division (cells 5). The *bud6* and *spa2* mutants might be defective in the partitioning at bud emergence, with all of the signal going to the bud tip (cell 2). Thus, there would be no signal molecules available at the mother bud neck to mark the division sites on mother and daughter cells at division (cells 5). Moreover, the patch of signal molecules at the distal pole of the daughter cell might be larger than normal (cells 5), accounting for the observations that in the mutant cells, first bud sites are less precisely positioned at the tips of the distal poles and second bud sites near the distal pole are generally not directly adjacent to the first bud site (see Results) (Fig. 3). The *bud8* mutant might also be defective in the partitioning at bud emergence, but in this case no signal molecules would go to the bud tip (cell 2), accounting for the observation that daughter cells make their first buds at their proximal poles and then continue to form buds adjacent either to the birth scar or to subsequent division sites at the proximal pole. The *bud9* mutant might partition signal molecules normally at bud emergence but then be defective in partitioning the molecules at the neck at cell division, resulting in a strong signal at the division site on the mother cell and a weak or nonexistent signal at the proximal pole of the daughter cell (cells 5). The mutant daughter cell would thus have an even stronger bias than normal for budding at its distal pole but would then be able to bud adjacent to previously used division sites at this pole in subsequent cycles (in contrast to the *bud6* and *spa2* mutants). The model shown here also appears to account for the observations that the *bud6 bud9* double mutant is able to position first bud sites at its distal pole (the *bud9* defect would have no effect in a cell that had already mispositioned signal due to the *bud6* defect) whereas the *bud6 bud8* double mutant buds randomly even in its first cell cycle (the opposing *bud6* and *bud8* defects at bud emergence might leave the cell unable to achieve any organized positioning of signal). However, it should be stressed that the model used here is just one of at least two plausible models for the positioning of the bipolar signal molecules in wild-type cells (15). Use of an alternative model might lead to different interpretations of the mutant phenotypes and thus to different predictions as to when and where the various gene products act. Discrimination between the possible models will probably require molecular evidence, such as localization of the proteins involved.

However, the localization of Spa2p (to the presumptive bud site on unbudded cells, to the tips of buds, and to the necks of cells undergoing cytokinesis) is suggestive of a role(s) in vegetative morphogenesis (69, 70), as is the effect of *spa2* mutations on cell shape and the size of the mother bud neck and bud scar (see Results). In addition, *SPA2* has been linked genetically to other genes whose products are clearly involved in vegetative morphogenesis, such as *CDC10* (27), which encodes a component of the neck filament assembly (41, 49); *BEM1* (17), which is important for polarity establishment (5, 11, 16); and *BCK1*/*SLK1* (17), which encodes a component of the protein kinase C-headed MAP kinase cascade involved in the maintenance of cell wall integrity during bud growth (reviewed in references 35 and 46).

We were surprised to isolate a *spa2* mutant in this study, because previous descriptions had suggested that *spa2* null mutations had only a modest effect on budding pattern and affected the axial as well as the bipolar pattern (27, 69, 70). However, Calcofluor staining of strains harboring *spa2*-Δ mutations revealed that they, like the *spa2-10* mutation identified here, randomize the budding of **a**/α cells but have little or no effect on the axial budding of **a** or α strains. Probably, the strong effect of *spa2* mutations on bipolar budding was not observed previously because the mutants select bud sites almost normally during the first one or two cell cycles (Fig. 3), an intriguing behavior that is discussed further below. As the localization of Spa2p coincides with that proposed for the bipolar budding-specific positional signals (see above and Fig. 6) (15), it is possible that Spa2p is a component of or plays a direct role in the localization of these signals.

BNI1 was originally identified on the basis of a mutation displaying synthetic lethality with a mutation in *CDC12*, which encodes another component of the neck filament assembly (26, 32, 49). A *bni1* null mutation, like the *bni1-2* mutation identified in this study, randomizes the budding of **a**/α cells (Fig. 3) but has no obvious effect on the axial budding pattern (26). *bni1* null mutations also significantly affect the structure of the mother bud neck and produce a partial defect in cytokinesis. Thus, it seems likely that Bni1p interacts with the neck filament proteins in the localization of the bipolar positional signals although not in the localization of the Bud3p/Bud4p-containing axial signal. Because even the first bud site is positioned randomly in a Bni1$^-$ strain (Fig. 3), it seems likely that Bni1p is involved in the placement of signals both at the distal pole of the daughter cell and at the division site. (For example, in the model of Fig. 6, Bni1p might be necessary for the initial localization of signal molecules to the presumptive bud site.)

The four novel genes identified in this study, *BUD6* to *BUD9*, may function exclusively or primarily in the bipolar-budding pathway. However, such a conclusion is not yet justified, for at least three reasons. First, we do not know whether the mutations identified here are null mutations. This seems likely for *BUD8* and *BUD9*, for which independent isolates have indistinguishable phenotypes, and less likely for *BUD7*, for which the cell-to-cell variations in budding pattern might reflect different levels of a partially active gene product. (For this reason, it seems prudent to defer detailed interpretation of the *bud7* phenotype until a bona fide null mutant is available.) Second, roles of the gene products in other aspects of growth and/or morphogenesis could be masked by functional redundancy with other genes. Third, we did observe some other modest phenotypic consequences (effects on cell shape or on growth rate under certain conditions) of the *bud6* to *bud9* mutations (see Results); these might reflect either roles of the

gene products in processes other than bud site selection or interactions with other proteins that have such roles. The latter interpretation would parallel one possible explanation of the lethality of *bud2* mutations in certain genetic backgrounds (7, 19).

Whether or not Bud6p, Bud8p, and Bud9p are involved exclusively in bipolar bud site selection, some speculations about their roles in this process appear justified by the available data. First, it is striking that in *bud6* or *spa2* mutant strains, daughter cells typically position their first buds almost normally at their distal poles (Fig. 3) and then bud more randomly in subsequent cell cycles (Fig. 1D, F, V, and X and Fig. 3). This suggests that Bud6p and Spa2p are components of or are involved in positioning the signal that normally marks the division site but not the signal at the distal tip of the daughter cell, as in the model shown in Fig. 6. Hence, a mutant *bud6* or *spa2* daughter cell would be able to bud at its (marked) distal pole, but in subsequent cell cycles, it would have no positional clues other than whatever portion of the distal-tip signal was still detectable after the first budding event.

Second, the *bud8* and *bud9* phenotypes can also be interpreted in terms of models for how the distal pole and division site become marked with bipolar positional signals. If the signals at the two sites involve any proteins that are different, *BUD8* might encode a component of the distal-pole signal (so that *bud8* mutant cells would be marked only at division sites, including the proximal pole of a daughter cell), and *BUD9* might encode a component of the division-site signal (so that only the distal tip of a daughter cell would be marked). However, this hypothesis does not seem attractive, at least for *BUD9*. It seems unlikely that different proteins would be involved in marking the daughter cell side and the mother cell side of the division site, but the continued budding of *bud9* mutant cells around their distal poles, at sites adjacent to previously used sites (Fig. 1I and AA), suggests that division sites must be marked on the mother cell side in such cells (note the quite different behavior of *bud6* and *spa2* mutant cells). Moreover, the ability of *bud8 bud9* double-mutant cells to bud consistently from their proximal poles (Fig. 4 and 5; Table 8) suggests that mutation of *BUD9* does not cause the loss of any essential component of the proximal-pole signal. Thus, we favor the hypothesis that Bud9p (and perhaps Bud8p as well, although the arguments are weaker) is involved in the proper positioning of signal molecules that are normally the same at both sites. For example, a *bud9* mutant might partition signal molecules incorrectly at the time of division, so that nearly all signal ends up on the mother cell side of the plane of cytokinesis (Fig. 6), whereas a *bud8* mutant might partition signal molecules incorrectly at the time of bud emergence, so that the distal pole would receive no signal (Fig. 6). In the *bud9* single mutant, the reduction in signal at the proximal pole of the daughter cell, coupled with the normal strong bias of daughter cells for budding at their distal poles (15), would result in budding exclusively from the distal pole, as observed. However, in the *bud8 bud9* double mutant, the absence of signal at the distal pole of a daughter cell would leave the weak signal at the proximal pole as the only positional clue, resulting in budding largely from the proximal pole, as observed (Fig. 4 and 5).

The epistasis of *bud6* and *spa2* to *bud8* and *bud9* is consistent with such models. Indeed, the model of Fig. 6 appears to rationalize even the difference between *bud6 bud8* and *bud6 bud9* strains in positioning of first bud sites (see the legend to Fig. 6). However, as other models also predict that mutations that randomize bud position would be epistatic to the *bud8* and *bud9* mutations, these results may be of limited value in discriminating among possible models.

While our studies were in progress, mutations in the *ACT1*, *RVS161*, *RVS167*, *SUR4*, and *FEN1* genes were also observed to affect the bipolar but not the axial budding pattern (2, 22, 23, 25, 67). It is interesting that mutations in *RVS161* and *RVS167* (as well as mutations in *ACT1*) appear to affect the structure of the actin cytoskeleton (2, 67) and that mutations in *RVS161*, *RVS167*, *SUR4*, and *FEN1* all appear to affect membrane lipid metabolism (20, 25, 44). These observations suggest that the positioning and/or function of the bipolar positional signals may depend on the actin cytoskeleton and on the structure of the plasma membrane. This hypothesis may help to explain the statistics of the mutant hunt described here: perhaps each of the "random" mutations fell into a different gene because there is a large set of genes (encoding proteins that affect the behavior of the actin cytoskeleton or plasma membrane lipid composition, as well as proteins dedicated to the bipolar-budding pathway) in which mutations can produce effects on bipolar but not on axial budding. In contrast, there may be relatively few genes whose products are involved so specifically in bipolar budding that mutations can produce a "unipolar" phenotype, explaining the repeated isolation of *bud8* and *bud9* mutations.

In conclusion, the studies reported here and recent observations by others appear to represent good first steps toward a molecular understanding of the mechanisms involved in bipolar bud site selection. Molecular analyses of *BUD6*, *BUD7*, *BUD8*, and *BUD9*, currently in progress, should also contribute to such an understanding.

ACKNOWLEDGMENTS

J.E.Z. and H.A.H. contributed equally to this work.

We thank E. Walsh for help in the initial mutant hunt; M. Aigle, A. Bender, S. Brown, J. Chant, P. Durrens, J. Fares, P. Hieter, L. Johnston, S. Lillie, M. Longtine, K. Madden, H.-O. Park, and M. Snyder for strains and/or plasmids; M. Aigle, C. Boone, D. Drubin, A. Durán, P. Durrens, I. Herskowitz, S. Sanders, and M. Snyder for communication of unpublished information; and members of our laboratory for encouragement, helpful discussions, and assistance.

This work was supported by NIH grant GM31006 and by the RJEG Trust. J.E.Z. was supported by NIH postdoctoral fellowship GM16478, and H.A.H. was supported by NIH training grant GM07092.

REFERENCES

1. **Adames, N., K. Blundell, M. N. Ashby, and C. Boone.** 1995. Role of yeast insulin-degrading enzyme homologs in propheromone processing and bud-site selection. Science **270:**464–467.
2. **Bauer, F., M. Urdaci, M. Aigle, and M. Crouzet.** 1993. Alteration of a yeast SH3 protein leads to conditional viability with defects in cytoskeletal and budding patterns. Mol. Cell. Biol. **13:**5070–5084.
3. **Bender, A.** 1993. Genetic evidence for the roles of the bud-site-selection genes *BUD5* and *BUD2* in control of the Rsr1p (Bud1p) GTPase in yeast. Proc. Natl. Acad. Sci. USA **90:**9926–9929.
4. **Bender, A., and J. R. Pringle.** 1989. Multicopy suppression of the *cdc24* budding defect in yeast by *CDC42* and three newly identified genes including the *ras*-related gene *RSR1*. Proc. Natl. Acad. Sci. USA **86:**9976–9980.
5. **Bender, A., and J. R. Pringle.** 1991. Use of a screen for synthetic lethal and multicopy suppressee mutants to identify two new genes involved in morphogenesis in *Saccharomyces cerevisiae*. Mol. Cell. Biol. **11:**1295–1305.
6. **Bender, A., and J. R. Pringle.** 1992. A Ser/Thr-rich multicopy suppressor of a *cdc24* bud emergence defect. Yeast **8:**315–323.
7. **Benton, B. K., A. H. Tinkelenberg, D. Jean, S. D. Plump, and F. R. Cross.** 1993. Genetic analysis of Cln/Cdc28 regulation of cell morphogenesis in budding yeast. EMBO J. **12:**5267–5275.
8. **Boone, C.** Personal communication.
9. **Botstein, D., S. C. Falco, S. E. Stewart, M. Brennan, S. Scherer, D. T. Stinchcomb, K. Struhl, and R. W. Davis.** 1979. Sterile host yeasts (SHY): a eukaryotic system of biological containment for recombinant DNA experiments. Gene **8:**17–24.
10. **Chant, J.** 1994. Cell polarity in yeast. Trends Genet. **10:**328–333.
11. **Chant, J., K. Corrado, J. R. Pringle, and I. Herskowitz.** 1991. Yeast *BUD5*, encoding a putative GDP-GTP exchange factor, is necessary for bud site selection and interacts with bud formation gene *BEM1*. Cell **65:**1213–1224.

12. **Chant, J., and I. Herskowitz.** 1991. Genetic control of bud site selection in yeast by a set of gene products that constitute a morphogenetic pathway. Cell **65:**1203–1212.
13. **Chant, J., M. Mischke, E. Mitchell, I. Herskowitz, and J. R. Pringle.** 1995. Role of Bud3p in producing the axial budding pattern of yeast. J. Cell Biol. **129:**767–778.
14. **Chant, J., and J. R. Pringle.** 1991. Budding and cell polarity in *Saccharomyces cerevisiae*. Curr. Opin. Genet. Dev. **1:**342–350.
15. **Chant, J., and J. R. Pringle.** 1995. Patterns of bud-site selection in the yeast *Saccharomyces cerevisiae*. J. Cell Biol. **129:**751–765.
16. **Chenevert, J., K. Corrado, A. Bender, J. R. Pringle, and I. Herskowitz.** 1992. A yeast gene (*BEM1*) necessary for cell polarization whose product contains two SH3 domains. Nature (London) **356:**77–79.
17. **Costigan, C., S. Gehrung, and M. Snyder.** 1992. A synthetic lethal screen identifies SLK1, a novel protein kinase homolog implicated in yeast cell morphogenesis and cell growth. Mol. Cell. Biol. **12:**1162–1178.
18. **Crouzet, M., M. Urdaci, L. Dulau, and M. Aigle.** 1991. Yeast mutant affected for viability upon nutrient starvation: characterization and cloning of the *RVS161* gene. Yeast **7:**727–743.
19. **Cvrčková, F., and K. Nasmyth.** 1993. Yeast G1 cyclins **CLN1** and **CLN2** and a GAP-like protein have a role in bud formation. EMBO J. **12:**5277–5286.
20. **Desfarges, L., P. Durrens, H. Juguelin, C. Cassagne, M. Bonneu, and M. Aigle.** 1993. Yeast mutants affected in viability upon starvation have a modified phospholipid composition. Yeast **9:**267–277.
21. **Drubin, D. G.** 1991. Development of cell polarity in budding yeast. Cell **65:** 1093–1096.
22. **Drubin, D. G.** Personal communication.
23. **Drubin, D. G., H. D. Jones, and K. F. Wertman.** 1993. Actin structure and function: roles in mitochondrial organization and morphogenesis in budding yeast and identification of the phalloidin-binding site. Mol. Biol. Cell **4:** 1277–1294.
24. **Durrens, P.** Personal communication.
25. **Durrens, P., E. Revardel, M. Bonneu, and M. Aigle.** 1995. Evidence for a branched pathway in the polarized cell division of *Saccharomyces cerevisiae*. Curr. Genet. **27:**213–216.
26. **Fares, H. F., M. S. Longtine, and J. R. Pringle.** Identification of genes involved in cell-cycle-dependent transcriptional activation and bud-site selection in yeast by screening for synthetic lethality with a *cdc12* septin mutation. Submitted for publication.
27. **Flescher, E. G., K. Madden, and M. Snyder.** 1993. Components required for cytokinesis are important for bud site selection in yeast. J. Cell Biol. **122:**373–386.
28. **Freifelder, D.** 1960. Bud position in *Saccharomyces cerevisiae*. J. Bacteriol. **80:**567–568.
29. **Fujita, A., C. Oka, Y. Arikawa, T. Katagai, A. Tonouchi, S. Kuhara, and Y. Misumi.** 1994. A yeast gene necessary for bud-site selection encodes a protein similar to insulin-degrading enzymes. Nature (London) **372:**567–570.
30. **Gehrung, S., and M. Snyder.** 1990. The *SPA2* gene of *Saccharomyces cerevisiae* is important for pheromone-induced morphogenesis and efficient mating. J. Cell Biol. **111:**1451–1464.
31. **Govindan, B., R. Bowser, and P. Novick.** 1995. The role of Myo2, a yeast class V myosin, in vesicular transport. J. Cell Biol. **128:**1055–1068.
32. **Haarer, B. K., and J. R. Pringle.** 1987. Immunofluorescence localization of the *Saccharomyces cerevisiae CDC12* gene product to the vicinity of the 10-nm filaments in the mother-bud neck. Mol. Cell. Biol. **7:**3678–3687.
33. **Harris, S. D., and J. R. Pringle.** 1991. Genetic analysis of *Saccharomyces cerevisiae* chromosome I: on the role of mutagen specificity in delimiting the set of genes identifiable using temperature-sensitive-lethal mutations. Genetics **127:**279–285.
34. **Hartwell, L. H., R. K. Mortimer, J. Culotti, and M. Culotti.** 1973. Genetic control of the cell division cycle in yeast. V. genetic analysis of *cdc* mutants. Genetics **74:**267–286.
35. **Herskowitz, I.** 1995. MAP kinase pathways in yeast: for mating and more. Cell **80:**187–197.
36. **Hicks, J. B., J. N. Strathern, and I. Herskowitz.** 1977. Interconversion of yeast mating types. III. Action of the homothallism (*HO*) gene in cells homozygous for the mating type locus. Genetics **85:**395–405.
37. **Hill, J. E., A. M. Myers, T. J. Koerner, and A. Tzagoloff.** 1986. Yeast/*E. coli* shuttle vectors with multiple unique restriction sites. Yeast **2:**163–167.
38. **Ito, H., Y. Fukuda, K. Murata, and A. Kimura.** 1983. Transformation of intact yeast cells treated with alkali cations. J. Bacteriol. **153:**163–168.
39. **Johnson, D. I., C. W. Jacobs, J. R. Pringle, L. C. Robinson, G. F. Carles, and M. V. Olson.** 1987. Mapping of the *Saccharomyces cerevisiae CDC3*, *CDC25*, and *CDC42* genes to chromosome XII by chromosome blotting and tetrad analysis. Yeast **3:**243–253.
40. **Johnson, D. I., and J. R. Pringle.** 1990. Molecular characterization of *CDC42*, a *Saccharomyces cerevisiae* gene involved in the development of cell polarity. J. Cell Biol. **111:**143–152.
41. **Kim, H. B., B. K. Haarer, and J. R. Pringle.** Unpublished results.
42. **Kohalmi, S. E., and B. A. Kunz.** 1988. Role of neighbouring bases and assessment of strand specificity in ethylmethanesulphonate and *N*-methyl-*N′*-nitro-*N*-nitrosoguanidine mutagenesis in the *SUP4-o* gene of *Saccharomyces cerevisiae*. J. Mol. Biol. **204:**561–568.
43. **Kunz, B. A., M. K. Pierce, J. R. A. Mis, and C. N. Giroux.** 1987. DNA sequence analysis of the mutational specificity of u.v. light in the *SUP4-o* gene of yeast. Mutagenesis **2:**445–453.
44. **Ladevèze, V., C. Marcireau, D. Delourme, and F. Karst.** 1993. General resistance to sterol biosynthesis inhibitors in *Saccharomyces cerevisiae*. Lipids **28:**907–912.
45. **Lawrence, C. W.** 1991. Classical mutagenesis techniques. Methods Enzymol. **194:**273–281.
46. **Levin, D., and B. Errede.** 1995. The proliferation of MAP kinase signalling pathways in yeast. Curr. Opin. Cell Biol. **7:**197–202.
47. **Lillie, S. H., and S. S. Brown.** 1994. Immunofluorescence localization of the unconventional myosin, Myo2p, and the putative kinesin-related protein, Smy1p, to the same regions of polarized growth in *Saccharomyces cerevisiae*. J. Cell Biol. **125:**825–842.
48. **Lillie, S. H., and J. R. Pringle.** 1980. Reserve carbohydrate metabolism in *Saccharomyces cerevisiae*: responses to nutrient limitation. J. Bacteriol. **143:**1384–1394.
49. **Longtine, M. S., D. J. DeMarini, M. L. Valencik, O. S. Al-Awar, H. Fares, C. Del Virgilio, and J. R. Pringle.** 1996. The septins: roles in cytokinesis and other processes. Curr. Opin. Cell Biol. **8:**106–119.
50. **Madden, K., and M. Snyder.** 1992. Specification of sites for polarized growth in *Saccharomyces cerevisiae* and the influence of external factors on site selection. Mol. Biol. Cell **3:**1025–1035.
51. **Mortimer, R. K., C. R. Contopoulou, and J. S. King.** 1992. Genetic and physical maps of *Saccharomyces cerevisiae*, edition 11. Yeast **8:**817–902.
52. **Park, H.-O., E. Bi, J. R. Pringle, and I. Herskowitz.** A GTPase cascade involved in determining cell polarity in yeast. Submitted for publication.
53. **Park, H.-O., J. Chant, and I. Herskowitz.** 1993. *BUD2* encodes a GTPase-activating protein for Bud1/Rsr1 necessary for proper bud-site selection in yeast. Nature (London) **365:**269–274.
54. **Powers, S., E. Gonzales, T. Christensen, J. Cubert, and D. Broek.** 1991. Functional cloning of *BUD5*, a *CDC25*-related gene from *S. cerevisiae* that can suppress a dominant-negative *RAS2* mutant. Cell **65:**1225–1231.
55. **Pringle, J. R.** 1991. Staining of bud scars and other cell wall chitin with Calcofluor. Methods Enzymol. **194:**732–735.
56. **Pringle, J. R., E. Bi, H. A. Harkins, J. E. Zahner, C. De Virgilio, J. Chant, K. Corrado, and H. Fares.** Establishment of cell polarity in yeast. Cold Spring Harbor Symp. Quant. Biol., in press.
57. **Pringle, J. R., and J.-R. Mor.** 1975. Methods for monitoring the growth of yeast cultures and for dealing with the clumping problem. Methods Cell Biol. **11:**131–168.
58. **Reid, B. J., and L. H. Hartwell.** 1977. Regulation of mating in the cell cycle of *Saccharomyces cerevisiae*. J. Cell Biol. **75:**355–365.
59. **Riles, L., J. E. Dutchik, A. Baktha, B. K. McCauley, E. C. Thayer, M. P. Leckie, V. V. Braden, J. E. Depke, and M. V. Olson.** 1993. Physical maps of the six smallest chromosomes of *Saccharomyces cerevisiae* at a resolution of 2.6 kilobase pairs. Genetics **134:**81–150.
60. **Rose, M. D., P. Novick, J. H. Thomas, D. Botstein, and G. R. Fink.** 1987. A *Saccharomyces cerevisiae* genomic plasmid bank based on a centromere-containing shuttle vector. Gene **60:**237–243.
61. **Rose, M. D., F. Winston, and P. Hieter.** 1991. Methods in yeast genetics: a laboratory course manual. Cold Spring Harbor Laboratory Press, Cold Spring Harbor, N.Y.
62. **Ruggieri, R., A. Bender, Y. Matsui, S. Powers, Y. Takai, J. R. Pringle, and K. Matsumoto.** 1992. *RSR1*, a *ras*-like gene homologous to K*rev*-1 (*smg21A*/*rap1A*): role in the development of cell polarity and interactions with the Ras pathway in *Saccharomyces cerevisiae*. Mol. Cell. Biol. **12:**758–766.
63. ***Saccharomyces* Genome Database.** 1995. Stanford University, Stanford, Calif.
64. **Sambrook, J., E. F. Fritsch, and T. Maniatis.** 1989. Molecular cloning: a laboratory manual, 2nd ed. Cold Spring Harbor Laboratory Press, Cold Spring Harbor, N.Y.
65. **Sanders, S. L., and I. Herskowitz.** Personal communication.
66. **Sherman, F., and J. Hicks.** 1991. Micromanipulation and dissection of asci. Methods Enzymol. **194:**21–37.
67. **Sivadon, P., F. Bauer, M. Aigle, and M. Crouzet.** 1995. Actin cytoskeleton and budding pattern are altered in the yeast *rvs161* mutant: the Rvs161 protein shares common domains with the brain protein amphiphysin. Mol. Gen. Genet. **246:**485–495.
68. **Sloat, B. F., A. Adams, and J. R. Pringle.** 1981. Roles of the *CDC24* gene product in cellular morphogenesis during the *Saccharomyces cerevisiae* cell cycle. J. Cell Biol. **89:**395–405.
69. **Snyder, M.** 1989. The *SPA2* protein of yeast localizes to sites of cell growth. J. Cell Biol. **108:**1419–1429.
70. **Snyder, M., S. Gehrung, and B. D. Page.** 1991. Studies concerning the temporal and genetic control of cell polarity in *Saccharomyces cerevisiae*. J. Cell Biol. **114:**515–532.
71. **Streiblová, E.** 1970. Study of scar formation in the life cycle of heterothallic *Saccharomyces cerevisiae*. Can. J. Microbiol. **16:**827–831.
72. **Welch, M. D., D. A. Holtzman, and D. G. Drubin.** 1994. The yeast actin cytoskeleton. Curr. Opin. Cell Biol. **6:**110–119.
73. **Winge, Ö.** 1935. On haplophase and diplophase in some Saccharomycetes. C. R. Trav. Lab. Carlsberg Ser. Physiol. **21:**77–111.
74. **Zheng, Y., A. Bender, and R. Cerione.** 1995. Interactions among proteins involved in bud-site selection and bud-site assembly in *Saccharomyces cerevisiae*. J. Biol. Chem. **270:**626–630.